

7466-EN-09

DTIC.

RESTRAINING POST-LIQUEFACTION FLOW DEFORMATIONS:

PHASE III

by

W.D. Liam Finn

June 1, 1995



United States Army

EUROPEAN RESEARCH OFFICE OF THE U.S. ARMY

London, England

Contract No.: N68171-94-C-9139

CORK GEOTECHNICS LTD.

Approved for Public Release: Distribution Unlimited

19950927 023

DTIC QUALITY INSPECTED 5

REPORT DOCUMENTATION PAGE			Form Approved OMB No 0704-0188	
<small>Public reporting burden for this collection of information is estimated to average 1 hour per response, including the time for reviewing instructions, searching existing data sources, gathering and maintaining the data needed, and completing and reviewing the collection of information. Send comments regarding this burden estimate or any other aspect of this collection of information, including suggestions for reducing this burden, to Washington Headquarters Service, Directorate for Information Operations and Reports, 1215 Jefferson Davis Highway, Suite 1204, Arlington, VA 22202-4302, and to the Office of Management and Budget, Paperwork Reduction Project (0704-0188), Washington, DC 20503.</small>				
1. AGENCY USE ONLY (Leave blank)	2. REPORT DATE June 1, 1995	3. REPORT TYPE AND DATES COVERED Draft Final: June 1994 to June 1995		
4. TITLE AND SUBTITLE RESTRAINING POST-LIQUEFACTION FLOW DEFORMATIONS: PHASE III		5. FUNDING NUMBERS N68171-94-C-9139		
6. AUTHOR(S) W.D. Liam Finn				
7. PERFORMING ORGANIZATION NAME(S) AND ADDRESS(ES) Cork Geotechnics Ltd. 7 Heffernan Terrace Castlemartyr County Cork, Ireland		8. PERFORMING ORGANIZATION REPORT NUMBER		
9. SPONSORING/MONITORING AGENCY NAME(S) AND ADDRESS(ES) European Research Office of the U.S. Army London, England		10. SPONSORING/MONITORING AGENCY REPORT NUMBER		
11. SUPPLEMENTARY NOTES				
12a. DISTRIBUTION / AVAILABILITY STATEMENT		12b. DISTRIBUTION CODE		
13. ABSTRACT (Maximum 200 words) A simplified nonlinear 3-D model is used to study the seismic response of pile groups. The method is validated for elastic analyses using existing exact solutions for small pile groups. Centrifuge data on the response of model pile groups in sand under strong shaking are used to verify the capability of the program to model the nonlinear response of pile groups. The program is used to evaluate a full-scale field test on a 6x6 pile group supporting a large transformer bank at the Duwamish Substation in Seattle, Washington. A novel feature of the method is that the time histories of lateral, rotational and coupled stiffnesses and corresponding damping factors for pile groups can be determined. This type of information is very useful when one is forced to select discrete springs and dashpots for use in commercial structural engineering programs for the analysis of structures on pile foundations such as bridges and tall buildings under earthquake loading.				
14. SUBJECT TERMS Rigid walls, Piles, Pile-soil interaction, 3-D model, Finite element, No rigid walls		15. NUMBER OF PAGES 52		
17. SECURITY CLASSIFICATION OF REPORT		18. SECURITY CLASSIFICATION OF THIS PAGE		16. PRICE CODE
17. SECURITY CLASSIFICATION OF REPORT		18. SECURITY CLASSIFICATION OF THIS PAGE		19. SECURITY CLASSIFICATION OF ABSTRACT
20. LIMITATION OF ABSTRACT				

RESTRAINING POST-LIQUEFACTION FLOW DEFORMATIONS:

PHASE III

by

W.D. Liam Finn

June 1, 1995

United States Army

Accession For	
NTIS	CRA&I <input checked="" type="checkbox"/>
DTIC	TAB <input checked="" type="checkbox"/>
Unannounced <input type="checkbox"/>	
Justification	
By	
Distribution /	
Availability Codes	
Dist	Avail and/or Special
A-1	

EUROPEAN RESEARCH OFFICE OF THE U.S. ARMY

London, England

Contract No.: N68171-94-C-9139

CORK GEOTECHNICS LTD.

Approved for Public Release: Distribution Unlimited

CHAPTER 1

INTRODUCTION

This report describes studies conducted for Phase III of the project "Restraining Post-Liquefaction Flow Deformations". To provide a context for this report, the background of the project will be reviewed briefly and some key findings from the previous two phases will be presented.

In Phase I of the project, (Finn, 1992) studies were focused on the use of piles to restrain flow deformations. This topic was of considerable interest to the US Army Corps of Engineers because pile-nailing of the upstream slope of Sardis Dam in Mississippi was being considered as an option for restraining sliding of the slope on a potentially liquefiable thin layer in the foundation (Finn et al., 1991).

The key factors controlling the feasibility and cost of installing piles to restrain flow deformations are pile length and spacing, stiffness and strength of unliquefied soils surrounding the piles, residual strength of liquefied soils, the geometry of the structure, and the intensity of shaking after liquefaction has occurred. The ability to analyze such a complex problem while taking into account nonlinear behaviour of soil, potentially large strain deformations in unremediated parts of the structure and a realistic interaction between piles and soil during both static and seismic loading is the essential requirement for determining the best location for the piles, an appropriate length and size and for categorizing the effects of soil properties. Very little is known about the behaviour of piles under these complex conditions.

The computer programs TARA-3 (Finn et al., 1986) and TARA-3FL (Finn and Yogendrakumar, 1989) were used in the Phase I studies to analyze the seismic response of the

pile-slope system and the post-liquefaction flow deformations. It was the first time such analyses had been performed. The findings of the Phase I studies were used to develop the design requirements for the piles for remediating Sardis Dam. The pile design resulted in very substantial savings in remediation costs compared to alternative proposals. The design would not have been feasible without the Phase I studies.

The studies for Sardis Dam could be conducted using the plane strain 2-D analyses in the TARA-3 suite of programs because remediation was necessary across a long longitudinal section of the dam. Where such conditions do not hold, 3-D analyses are necessary.

Generally, full 3-D nonlinear dynamic analysis of pile groups is not a feasible proposition for engineering practice at present. It makes impractical demands on computational speed and capacity and renders the extension to dynamic effective stress analysis extremely difficult. Full 3-D analysis also inhibits the detailed parametric studies which are so important in exploring cost-efficient remediation options. In Phase II studies, a simplified model for the 3-D soil continuum under horizontal shaking by vertically propagating shear waves was used to overcome these difficulties. This simplified 3-D model (Wu, 1994) captured the significant motions and stresses in foundation soils with acceptable accuracy during ground shaking and provided the basis for significant advances in the seismic analysis of piles.

The computational model of the foundation soil layers was formulated in terms of finite elements and embedded piles were modelled by the incorporation of beam elements. This new model was incorporated in the computer program PILE-3D by Wu and Finn (1994). Solutions can be obtained for both elastic and nonlinear soil response. Nonlinear response is modelled by maintaining compatibility between shear strains and effective moduli and damping throughout the

dynamic analysis. Seismic response analyses in Phase II were restricted to single piles for both elastic and nonlinear material conditions.

The PILE-3D program was validated for elastic response using existing exact elastic solutions. The soil continuum model was validated using Wood's (1973) exact solution for dynamic pressures against rigid walls. The pile-soil model was validated by comparing elastic pile impedances for single piles computed by PILE-3D with those computed by Kaynia and Kausel (1982) using full 3-D continuum equations. Agreement between PILE-3D solutions and the more exact solution is very good.

The model also simulated successfully the response of a full scale Franki type pile to low level forced vibration in a field test. The test was conducted at the University of British Columbia Pile Research Facility by Sy and Siu (1992).

In the nonlinear mode, the model was validated for single pile response using data from strong shaking tests on single pile foundations conducted on the centrifuge at the California Institute of Technology (Gohl, 1991). The important aspects of acceleration and moment time histories were simulated well by the model and the distribution of peak moments along the pile were within 6% of the measured moments.

The computational time for conducting 3-D analyses was greatly reduced by using the simplified model. Thus, the main objective of the Phase II studies was achieved.

In Phase III, the simplified model has been used to study the seismic response of pile groups. The same procedure used in Phase II was followed. First, the method was validated for elastic analyses using existing exact solutions for small pile groups by Kaynia and Kausel (1982). Data on the response of model pile groups in sand under strong shaking obtained from centrifuge

tests (Gohl, 1991) were used to verify the capability of the program to model nonlinear response of pile groups.

This report is restricted to describing the evolution and validation of a proposed simplified 3-D method of analysis of the dynamic response of pile groups that greatly reduces the computational demands for solving practical problems. It is not a state-of-the-art study of the dynamic response of pile foundations. References to the literature are restricted primarily to case studies used for validation.

Structure of Report

The theoretical development of the simplified 3-D model is presented first and extended from single piles to pile groups. This extension involves the adequate modelling of the vertical and rocking modes of a pile group within the constraints of the simplified 3-D model. It is necessary to repeat some of the theoretical formulations from the Phase II report here in order to make the present report complete in itself.

The dynamic impedances of a 2×2 pile groups are determined for elastic response and compared with exact 3-D solutions by Kaynia and Kausel (1982) to validate the model, especially the rocking mode. Then the program is used to evaluate a full scale field test on a 6×6 pile group supporting a large transformer bank at the Duwamish substation in Seattle, Washington.

Data from centrifuge tests on a 2×2 pile group under strong shaking conducted at the California Institute of Technology in 1991 are used to validate the capacity of the program to model the nonlinear response of pile foundations.

The report concludes by making some recommendations for further research.

CHAPTER 2

DYNAMIC RESPONSE OF PILES GROUPS: FINITE ELEMENT FORMULATION

Equations of Motion for Soil-Pile System

Under vertically propagating shear waves, the foundation soils undergo mainly shearing deformations in horizontal planes except in the area near the pile where extensive compressive deformations develop in the direction of shaking. The compressive deformations also generate additional shearing deformations along the sides of the pile because of the limited extent of the pile cross-section. In light of these observations, assumptions are made that dynamic motions of foundation soils are governed by compressive stresses in the direction of shaking, y , and two kinds of shear stresses.

Let v represent the horizontal displacement of the soil in the direction of shaking, y (Fig. 2.1). Applying dynamic equilibrium in the y -direction, the dynamic equation for damped free vibration of the soil continuum is written as

$$G^* \frac{\partial^2 v}{\partial x^2} + \theta G^* \frac{\partial^2 v}{\partial y^2} + G^* \frac{\partial^2 v}{\partial z^2} = \rho_s \frac{\partial^2 v}{\partial t^2} \quad (2.1)$$

where G^* is the complex shear modulus, ρ_s is the mass density of the soil, $\theta = 2/(1-\mu)$ and μ is the Poisson's ratio. The complex shear modulus $G^* = G(1+i2\lambda)$ where G is the shear modulus and λ is the viscous damping ratio equivalent to the hysteretic damping in the soil.

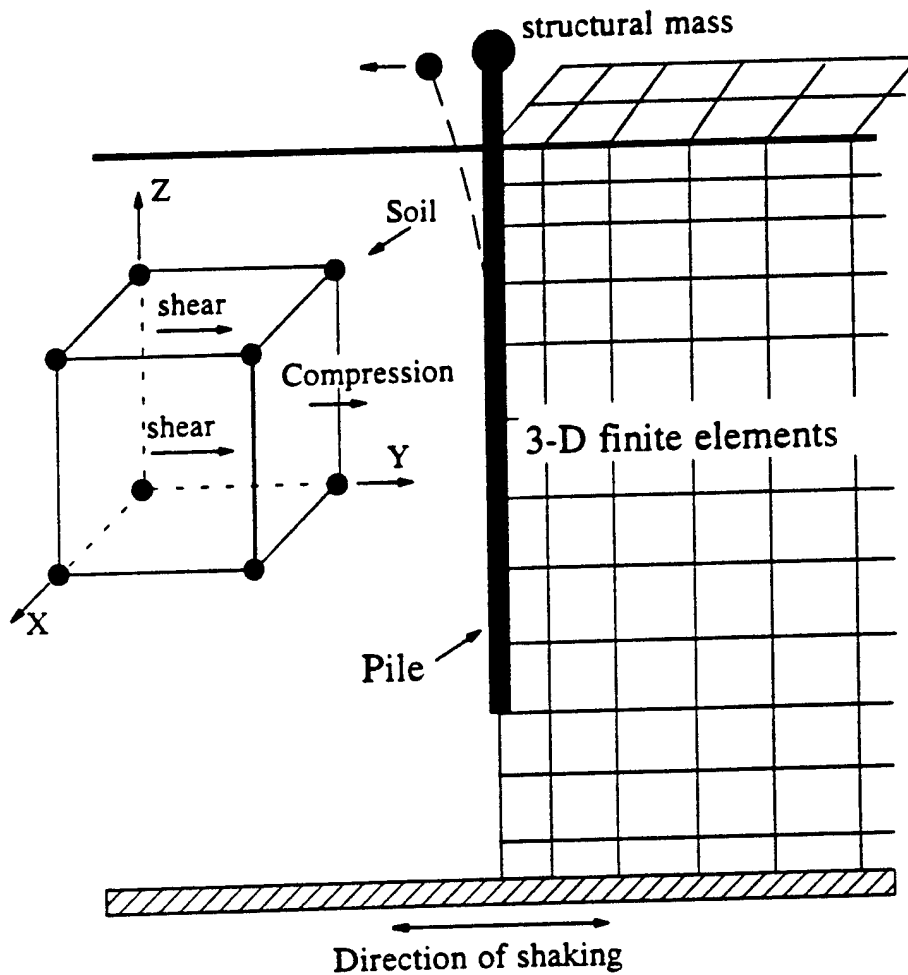


Fig. 2.1. Important stresses generated by pile-soil interaction during horizontal excitation by shear waves.

The term $\rho_s \frac{\partial^2 v}{\partial t^2}$ is the inertial force due to soil acceleration. The compressive force in the direction of motion is $\theta G \frac{\partial^2 v}{\partial y^2}$. The term $G \frac{\partial^2 v}{\partial z^2}$ is the shear force in the xOy plane and $G \frac{\partial^2 v}{\partial x^2}$ is the shear force in yOz plane.

Piles are modelled using ordinary Eulerian beam theory. Only the bending moment in the plane of shaking (yOz) is included. This consideration is appropriate in the case of earthquake loading for single piles.

The dynamic equation of flexural motion for a vertical pile is written as

$$E_p I_x \frac{\partial^4 v}{\partial z^2} = \rho_p A \frac{\partial^2 v}{\partial t^2} \quad (2.2)$$

where A , $E_p I_x$ and ρ_p are the cross-sectional area, flexural rigidity and the mass density of the pile, respectively.

Finite Element Formulation of Equations of Motion

The 3-dimensional soil continuum is divided into a number of 3-D finite elements of the type shown in Fig. 2.2. The displacement field in each element is specified by the nodal displacements and appropriate shape functions. A linear displacement field in the soil element is used because of its simplicity and effectiveness.

The displacement vector $v(x,y,z)$ is expressed as

$$v(x,y,z) = \sum N_i \times v_i, \dots i = 1,8 \quad (2.3)$$

where N_i is a shape function, and v_i is a nodal displacement.

Applying the Galerkin's weighted residual procedure to Eq. 2.1, the complex valued stiffness matrix of the soil element is determined

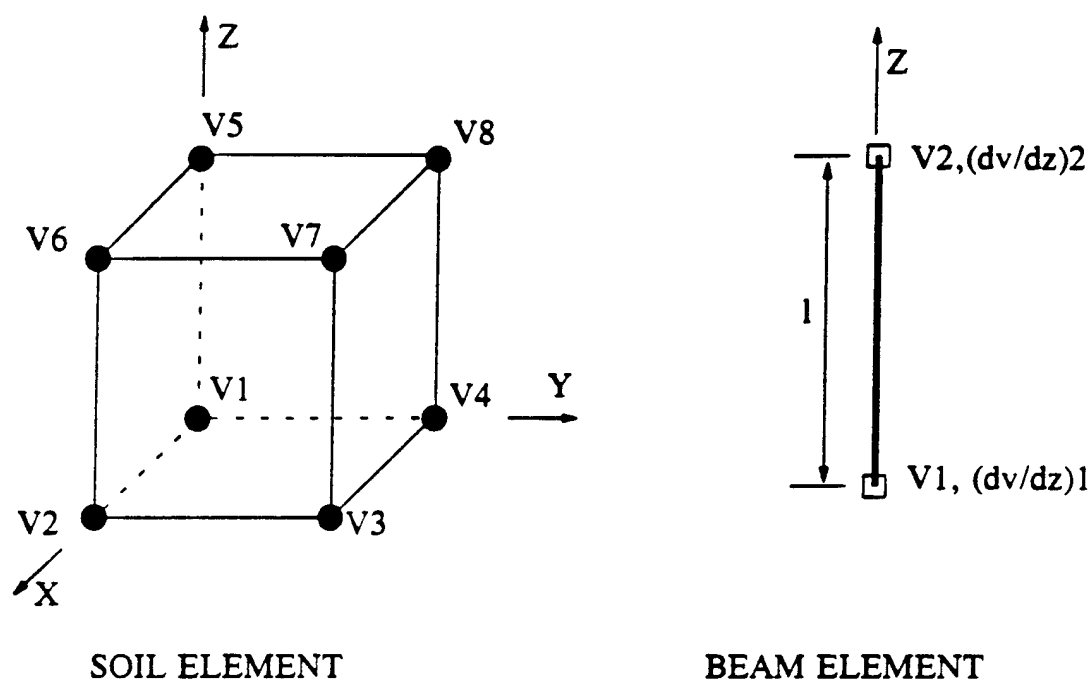


Fig. 2.2: Finite elements used for soil continuum and pile.

$$[K^*]_{\text{soil}} = \iiint \left(\theta G^* \frac{\partial N_i}{\partial y} \frac{\partial N_j}{\partial y} + G^* \frac{\partial N_i}{\partial x} \frac{\partial N_j}{\partial x} + G^* \frac{\partial N_i}{\partial z} \frac{\partial N_j}{\partial z} \right) dx dy dz \quad (2.4)$$

For a vertical beam element, (Fig. 2.2) the stiffness matrix is

$$[K]_{\text{pile}} = \frac{E_p I_x}{l^3} \begin{bmatrix} 12 & 6l & -12 & 6l \\ 6l & 4l^2 & -6l & 2l^2 \\ -12 & -6l & 12 & -6l \\ 6l & 2l^2 & -6l & 4l^2 \end{bmatrix} \quad (2.5)$$

The two nodes in a vertical beam element are shared with adjacent soil elements, thus coupling the pile and the soil. The stiffness of a node, therefore, is comprised of stiffness contributions from both the pile and the soil.

Consistent mass matrices are used for both soil elements and pile elements. The consistent mass matrix for a soil element is

$$[M]_{\text{soil}} = \iiint \rho_s \cdot N_i N_j \cdot dx dy dz \quad (2.6)$$

The consistent mass matrix for a pile element is written as

$$[M]_{\text{pile}} = \frac{\rho_p A \ell}{420} \begin{bmatrix} 156 & 22\ell & 54 & -13\ell \\ 22\ell & 4\ell^2 & 13\ell & -3\ell^2 \\ 54 & 13\ell & 156 & -22\ell \\ -13\ell & -3\ell^2 & -22\ell & 4\ell^2 \end{bmatrix} \quad (2.7)$$

The global stiffness matrix $[K^*]$ and the global mass matrix $[M]$ are constructed by standard routines from the element stiffnesses and masses.

Radiation damping is modelled by using a set of viscous dashpots along the pile shaft. The damping force F_d per unit length along the pile is considered proportional to the velocity and is given by

$$F_d = c_r \cdot \frac{\partial v}{\partial t} \quad (2.8)$$

where c_r is the radiation damping coefficient.

Gazetas et al. (1993) proposed simple expressions for the radiation damping coefficients for vertical (c_z) and horizontal (c_x) motions,

$$c_x = 6\rho_s V_s d a_0^{-0.25} \quad (2.9)$$

and

$$c_z = \rho_s V_s d a_0^{-0.25} \quad (2.10)$$

in which d is the pile diameter, V_s = shear wave velocity in the soil, and $a_0 = \omega d/V_s$, where ω = circular frequency.

The element radiation damping matrix $[C]_{\text{elem}}$ is then given by,

$$[C]_{\text{elem}} = \frac{c_r \ell}{420} \begin{bmatrix} 156 & 22\ell & 54 & -13\ell \\ 22\ell & 4\ell^2 & 13\ell & -3\ell^2 \\ 54 & 13\ell & 156 & -22\ell \\ -13\ell & -3\ell^2 & -22\ell & 4\ell^2 \end{bmatrix} \quad (2.11)$$

This is equivalent to assuming that the damping matrix is proportional to the mass matrix. The appropriate value of c_r is used for the direction of motion under consideration; c_z for vertical, c_x for horizontal.

The global dynamic equilibrium equation in matrix form is now,

$$[M]\{\ddot{v}\} + [C]\{\dot{v}\} + [K^*]\{v\} = \{P(t)\} \quad (2.12)$$

in which $\{\ddot{v}\}$, $\{\dot{v}\}$ and $\{v\}$ are the nodal accelerations, velocities and displacements, respectively, and $\{P(t)\}$ are external dynamic loads.

Equation 2.11 applies directly to the horizontal excitation of single piles. However, in the case of pile groups connected by a pile cap, the horizontal motion of the pile cap is coupled with the rocking motion of the group. Therefore, before any pile group connected by a pile cap can be analyzed, the PILE-3D analysis must be extended to include rocking motions.

CHAPTER 3

IMPEDANCES OF SINGLE PILES AND PILE GROUPS

In engineering practice, it is not common to analyze, as a unit, a structure and its pile foundation. This is particularly true for structures with multiple seismic inputs such as multi-span bridges. Generally, the effects of the pile foundations are modelled in the analysis by adding springs and dampers to the structural supports, which characterize the stiffness and damping provided by the pile foundations. The combination of stiffness and damping associated with any particular direction of motion is called the pile group impedance for that direction of motion.

The derivation of the impedances of single piles was discussed in detail in the Phase II report (Finn, 1994). The definitions of impedances for single piles are presented again here to facilitate the understanding of the corresponding definitions for pile groups.

Single Pile Impedances

The impedances K_{ij} are defined as the amplitudes of harmonic forces (or moments) that have to be applied at the pile head in order to generate a harmonic motion with a unit amplitude in the direction of the specified degree of freedom (Novak, 1991) as shown in Fig. 3.1.

The pile head impedances are defined as follows:

- K_{vv} : the complex-valued horizontal force applied at the pile head which is required to generate unit horizontal displacement ($v = 1.0$) at the pile head while the pile head is fixed against rotation ($\theta = 0$).
- $K_{v\theta}$: the complex-valued moment generated by unit lateral displacement ($v = 1.0$) at the pile head while the pile head is fixed against rotation ($\theta = 0$).

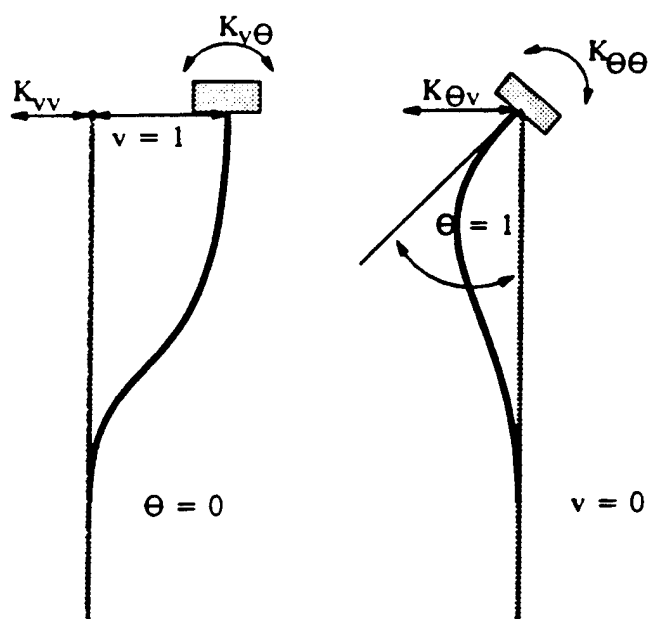


Fig. 3.1: Pile head impedances.

$K_{\theta\theta}$: the complex-valued moment required at the pile cap to generate unit rotation of the pile head ($\theta = 1.0$) while the pile head is fixed against lateral displacement ($v = 0$).

Since the pile head impedances K_{vv} , $K_{v\theta}$, $K_{\theta\theta}$ are complex valued, they are usually expressed by their real and imaginary parts as

$$K_{ij} = k_{ij} + i \cdot C_{ij} = k_{ij} + i \cdot \omega c_{ij} \quad (3.1)$$

in which k_{ij} and C_{ij} are the real and imaginary parts of the complex impedance, respectively, and are usually referred as the stiffness and damping at the pile head, $i = \sqrt{-1}$; $c_{ij} = C_{ij} / \omega$ = coefficient of equivalent viscous damping; and ω is the circular frequency of the applied load. All

the parameters in Eq. 3.1 are dependent on frequency ω . Determination of the pile impedances requires solutions of the equations of motion for harmonic loading.

Under harmonic loading $P(t) = P_0 e^{i\omega t}$, the displacement vector is of the form $v = v_0 e^{i\omega t}$, and Eq. 2.11 is rewritten as

$$\{[K] + i \cdot \omega[C] - \omega^2[M]\} \{v_0\} = \{P_0\} \quad (3.2)$$

or

$$[K]_{\text{global}} \{v_0\} = \{P_0\} \quad (3.3)$$

where

$$[K]_{\text{global}} = [K] + i \cdot \omega[C] - \omega^2[M] \quad (3.4)$$

The pile head impedances K_{vv} , $K_{v\theta}$ and $K_{\theta\theta}$ can be obtained using Eq. 3.3 by applying appropriate loading and fixity conditions at the pile head. These analyses are conducted using the program PILIMP (Wu and Finn, 1994). The determination of pile stiffness and damping factors from such analyses was described in the Phase II report by Finn (1994).

Pile Group Impedances

The pile cap impedances, K_{vv} , $K_{v\theta}$, and $K_{\theta\theta}$ for a pile group are defined in the same way as the pile head impedances for single piles. It is only necessary to substitute the words "pile cap" instead of "pile head" in the definitions given earlier for single piles.

The impedance of a group of N piles, associated with a particular degree of freedom, is not given by N times the corresponding impedance of a single pile because of interaction between the piles in the group. Therefore, pile group impedances must be obtained by solving the equations of motion of the group under the action of harmonic forces sufficient to generate unit generalized displacements at the pile cap.

During even horizontal excitation, a heavy pile cap attached to a pile group will undergo rocking as well as horizontal motions. The rocking is resisted mainly by the vertical resistance of the piles. Therefore, in order to determine group impedances, PILE-3D must be formulated also for vertical motions. This is done in the next chapter.

CHAPTER 4

DYNAMIC ELASTIC ROCKING IMPEDANCE OF PILE GROUPS

Introduction

The rocking impedance of a pile group reflects the resistance to rotation of the pile cap connecting the foundation piles. The rocking impedance K_{rr} of a pile group is defined as the resisting moment of the pile cap to a unit rotation. If the piles are pinned to the pile cap, as in Fig. 4.1, this resisting moment is generated only by the axial forces at all the pile heads about the axis of rotation

$$K_{rr} = \sum r_i \cdot F_i \quad (4.1)$$

where r_i is the distance between the axis of rotation and pile i , and F_i is the axial force at the head of pile i when $\theta_{cap} = 1.0$

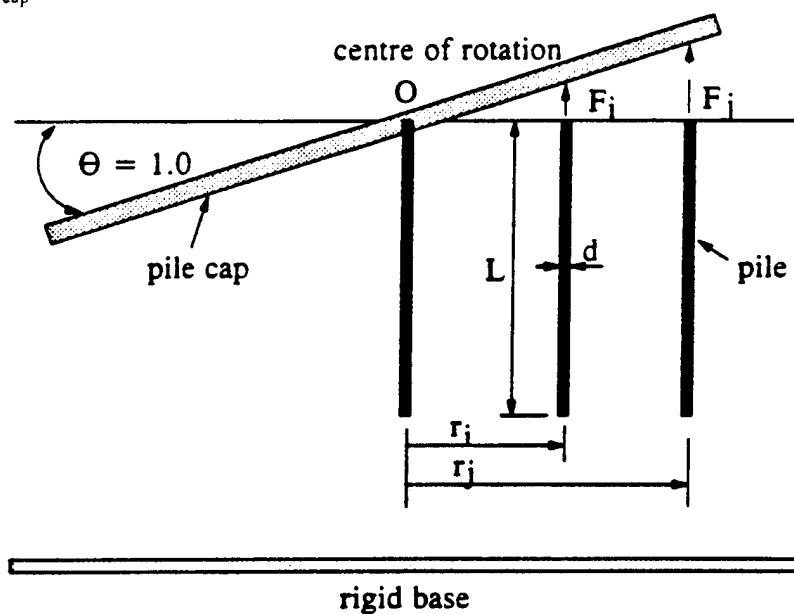


Fig. 4.1: Pile foundation under vertical loads

In order to determine the rocking impedance, it is necessary to evaluate the axial forces in Eq. 4.1 caused by the unit rotation of the pile cap. This is done by applying the program PILE-3D in the vertical direction.

Dynamic equation of motion in the vertical direction

Under vertically propagating compression waves, the soil medium undergoes mainly axial deformations in the vertical direction. In the two perpendicular horizontal directions, shearing deformations are generated due to the internal friction of the soil. Although axial stresses occur in the two horizontal directions also, the assumption is made that these dynamic normal stresses are small and can be ignored.

The composition of forces in a soil element near a vertical pile is shown in Fig. 4.2. Let w represents the displacement of soil in the vertical direction. The axial force in Z direction is

$\theta G \frac{\partial^2 w}{\partial z^2}$. The shear force in YOZ plane is $G \frac{\partial^2 w}{\partial x^2}$, and the shear force in XOZ plane is $G \frac{\partial^2 w}{\partial y^2}$;

the two shear waves propagate in X direction and Y direction, respectively. The inertia force is

$\rho_s \frac{\partial^2 w}{\partial t^2}$. Applying dynamic equilibrium in Z-direction, the dynamic governing equation under

free vibration of the soil continuum is written as

$$G^* \frac{\partial^2 w}{\partial x^2} + G^* \frac{\partial^2 w}{\partial y^2} + \theta_z G^* \frac{\partial^2 w}{\partial z^2} = \rho_s \frac{\partial^2 w}{\partial t^2} \quad (4.2)$$

where G^* is the complex shear modulus, ρ_s is the mass density of soil, and $\theta_z = 2(1+\mu)$.

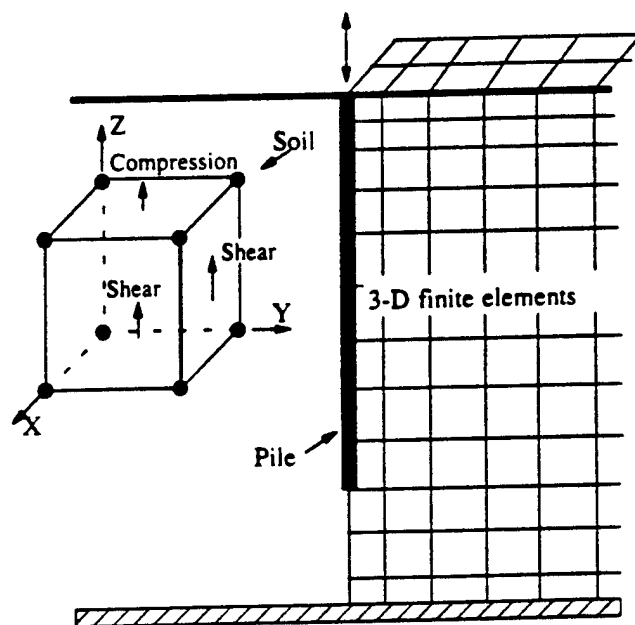


Fig. 4.2: Important stresses generated by pile-soil interaction during vertical excitation.

The dynamic equation for free undamped vertical motion of a pile is given by

$$E_p A \frac{\partial^2 w}{\partial z^2} = \rho_p \frac{\partial^2 w}{\partial t^2} \quad (4.3)$$

where $E_p A$ is the rigidity of the pile, and ρ_p is the mass density of the pile.

Soil-pile interaction is modelled by enforcing displacement compatibility between the pile and the soil.

For a vertical beam element, according Eq. 4.3, the stiffness matrix is

$$[K]_{\text{pile}} = \frac{E_p A}{\ell} \begin{bmatrix} 1 & -1 \\ -1 & 1 \end{bmatrix} \quad (4.4)$$

The complex stiffness of a 3-D soil element is given by Eq. (2.4). The consistent mass matrix for a vertical pile element under vertical motion is written as

$$[M]_{\text{pile}} = \frac{\rho_p \ell A}{6} \begin{bmatrix} 2 & 1 \\ 1 & 2 \end{bmatrix} \quad (4.5)$$

where A is the area of the cross-section of the pile.

The radiation damping matrix for a pile element is given by

$$[C]_{\text{pile}} = \frac{c_z \ell}{6} \begin{bmatrix} 2 & 1 \\ 1 & 2 \end{bmatrix} \quad (4.6)$$

The global dynamic equilibrium equation, in the vertical direction in matrix form is given by,

$$[M]\{\ddot{w}\} + [C]\{\dot{w}\} + [K^*]\{w\} = \{P(t)\} \quad (4.7)$$

in which $\{\ddot{w}\}$, $\{\dot{w}\}$ and $\{w\}$ are the nodal accelerations, velocities and displacements, respectively, in the vertical direction, and $P(t)$ is the external dynamic loading. $[M]$, $[C]$ and $[K^*]$ are the global mass damping and complex stiffness matrices, formed using the same procedures as for the case of horizontal motion. The $[M]_{\text{soil}}$ and $[K]_{\text{soil}}$ components of $[M]$ and $[K^*]$ are given by Eq. (2.6) and Eq. (2.4), respectively.

Determination of rocking impedance

In order to evaluate the rocking impedance of a pile group, harmonic forces $P(t) = P_0 e^{i\omega t}$ are applied to the pile cap which generate harmonic displacements $w = w_0 e^{i\omega t}$. On substituting for w in Eq. (4.7), the equation of motion reduces to

$$[K]_{\text{global}} \{w_0\} = \{P_0\} \quad (4.8)$$

where

$$[K]_{\text{global}} = \{[K] + i \cdot \omega [C] - \omega^2 [M]\} \quad (4.9)$$

is a complex banded matrix.

Since the vertical displacements at the pile heads $\{w_1^p, w_2^p, \dots, w_m^p\}^T$, are known for a unit rotation of the pile cap, the axial forces $\{F_1, F_2, \dots, F_m\}^T$ may be determined from

$$\begin{bmatrix} K_{nn} & K_{nm} \\ K_{mn} & K_{mm} \end{bmatrix} \begin{Bmatrix} w_1 \\ w_2 \\ \vdots \\ w_n \\ w_1^p \\ \vdots \\ w_m^p \end{Bmatrix} = \begin{Bmatrix} 0 \\ 0 \\ \vdots \\ 0 \\ F_1 \\ \vdots \\ F_m \end{Bmatrix} \quad (4.10)$$

where K_{nn} , K_{nm} , K_{mn} , and K_{mm} are sub-matrices of the global matrix K_{global} , and $\{w_1, w_2, \dots, w_n\}^T$ are vertical displacements at nodes other than the pile heads. The pile head axial forces $\{F_1, F_2, \dots, F_m\}^T$ can be determined if the displacements $\{w_1, w_2, \dots, w_n\}^T$ are known. Applying the matrix separation technique to Eq. 4.10 yields

$$K_{nn} \begin{Bmatrix} w_1 \\ \vdots \\ w_m \end{Bmatrix} + K_{nm} \begin{Bmatrix} w_1^p \\ \vdots \\ w_m^p \end{Bmatrix} = \{0\} \quad (4.11)$$

and

$$\begin{Bmatrix} F_1 \\ \vdots \\ F_m \end{Bmatrix} = K_{mn} \begin{Bmatrix} w_1 \\ \vdots \\ w_n \end{Bmatrix} + K_{mm} \begin{Bmatrix} w_1^p \\ \vdots \\ w_m^p \end{Bmatrix} \quad (4.12)$$

After the displacement vector $\{w_1, w_2, \dots, w_n\}^T$ is computed from Eq. 4.11, the pile head axial force vector $\{F_1, \dots, F_m\}$ is then determined using Eq. 4.12. Now the rocking impedances of the pile group are evaluated using Eq. 4.1, if the piles are pinned to the pile cap. If the piles are fixed to the pile cap, then the individual pile head rotational stiffnesses, $k_{\theta\theta}$, should be added to the stiffness computed using Eq. 4.1. This procedure is incorporated in the program PILIMP (Wu and Finn, 1994).

Vertical Impedance of a Pile Group

The vertical impedance of a pile group is obtained by applying harmonic forces $P(t) = P_0 e^{i\omega t}$, to the pile cap which generate unit vertical displacement of the pile cap. Thus, all pile

heads undergo uniform vertical displacement. Therefore, in this case, as in the case of rocking, since the pile head displacements are known, the associated complex forces and hence the impedances can be determined by the same matrix technique used to determine rocking stiffness. These calculations conducted using the program PILIMP (Wu and Finn, 1994).

CHAPTER 5

ELASTIC RESPONSE OF PILE GROUP: VALIDATION STUDIES

The dynamic impedances of small pile groups in a half-space elastic soil medium were calculated by Kaynia and Kausel (1982) using full 3-D elastic analysis. Their results were used to validate the pile-group analyses by PILE-3D. As a typical example of the degree of comparison between the results of full 3-D elastic analysis and the results from the quasi 3-D PILE-3D analysis, the results from the analysis of a four-pile group will be presented. The pile group is shown in Fig. 5.1. The rigid pile cap is rigidly connected to the four pile heads as shown in Fig. 5.1. A stiffness ratio of the pile and soil $E_p/E_s = 1,000$ is used, where E_p and E_s are the Young's moduli of the pile and soil, respectively. The mass density ratio $\rho_s/\rho_p = 0.7$ is used, where ρ_s and ρ_p are the mass densities of the soil and pile, respectively.

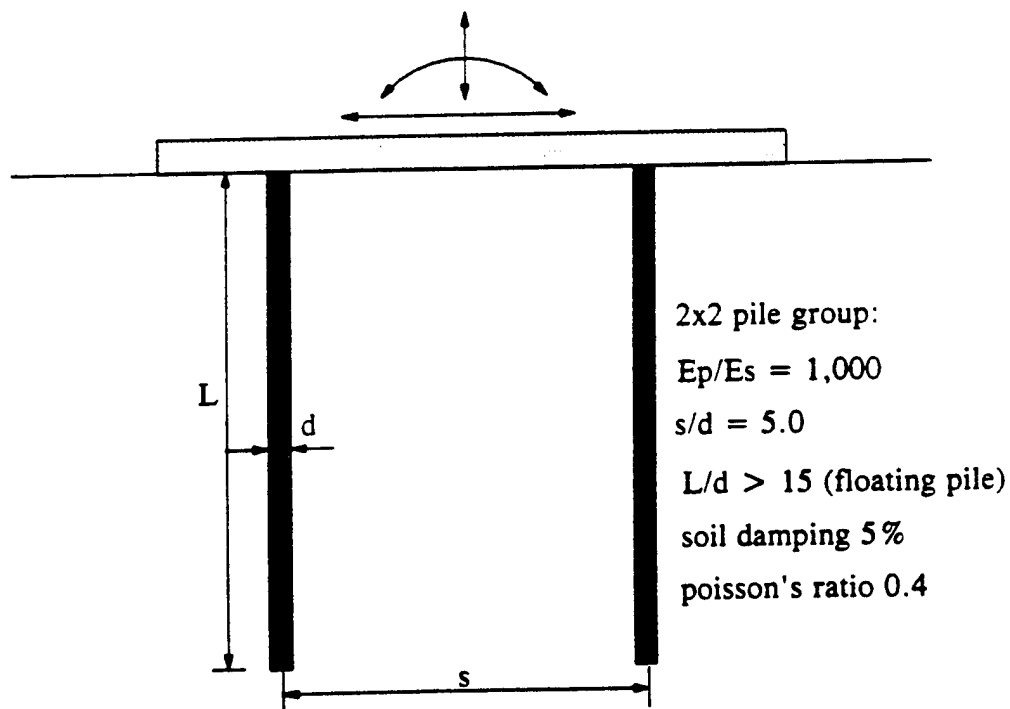


Fig. 5.1: A 2x2 pile foundation with rigid pile cap.

In the PILE-3D analysis, the half-space medium was represented by a finite element mesh with a rigid base at a depth of $5L$ (L = length of pile) beyond the tip of the pile. The dynamic impedances were evaluated at the bottom of the pile cap. In order to compare the dynamic impedances calculated using PILIMP (Wu and Finn, 1994), with the results of the Kaynia and Kausel (1982) study, the dynamic impedances of the pile group are first normalized to the static stiffness of the pile group expressed as the stiffness of a single pile times the number of piles in the group. These normalized dynamic impedances are called the dynamic interaction factors.

These factors are defined as follows

$$\alpha_{vv} = \frac{K_{vv}}{N \cdot k_{vv}^0} \quad (5.1)$$

$$\alpha_{v\theta} = \frac{K_{v\theta}}{N \cdot k_{v\theta}^0} \quad (5.2)$$

$$\alpha_{\theta\theta} = \frac{K_{\theta\theta}}{N \cdot k_{\theta\theta}^0} \quad (5.3)$$

in which $k_{vv}^0, k_{v\theta}^0, k_{\theta\theta}^0$ are static stiffnesses of a single pile identical to those in the pile group that is placed alone in the same soil medium, and N is the number of piles in the pile group. K_{vv} , $K_{v\theta}$ and $K_{\theta\theta}$ are the computed vertical, cross and rocking stiffnesses of the pile group.

For pile groups with a pile cap, $K_{\theta\theta}$ is the total rotational impedance of the pile cap including the resisting moments due to the axial forces in the piles and the individual rotational stiffness at the head of each pile, if the piles are rigidly attached to the pile cap. If the connection

is pinned, then $K_{\theta\theta}$ is due only to the axial forces in the piles. The normalization factor used here for a pile cap is $(N \cdot \sum r_i^2 k_{zz}^0)$, where k_{zz}^0 is the static vertical stiffness of a single pile placed alone in the same soil medium.

In order to present the results graphically, the complex valued dynamic interaction factors α_{ij} are separated into their real and imaginary parts, α_{ij} (stiffness) and α_{ij} (damping), respectively. The computed dynamic interaction factor α_{vv} (stiffness) is compared in Fig. 5.2(a) with that calculated by Kaynia and Kausel (1982) using full 3-D analysis. There is very good agreement between the two estimates of stiffness. Good agreement is also found between the damping interaction factors obtained by the two methods (Fig. 5.2b).

Similar comparisons are shown for the rotational impedance factors: $\alpha_{\theta\theta}$ (rotational stiffness) and $\alpha_{\theta\theta}$ (damping), in Fig. 5.3(a) and Fig. 5.3(b), respectively. In this figure, the normalization factor $(N \cdot \sum r_i^2 k_{zz}^0)$ is represented by A.

The proposed model appears to simulate well the dynamic characteristics of pile groups when the response is elastic. The agreement would be improved by using a finer mesh but for practical analysis it is necessary to strike a balance between accuracy and computing time.

Field vibration tests of a six pile group, at low amplitudes of excitation, provided the opportunity to verify the reliability of the proposed model under field conditions. This validation study is described in the next chapter.

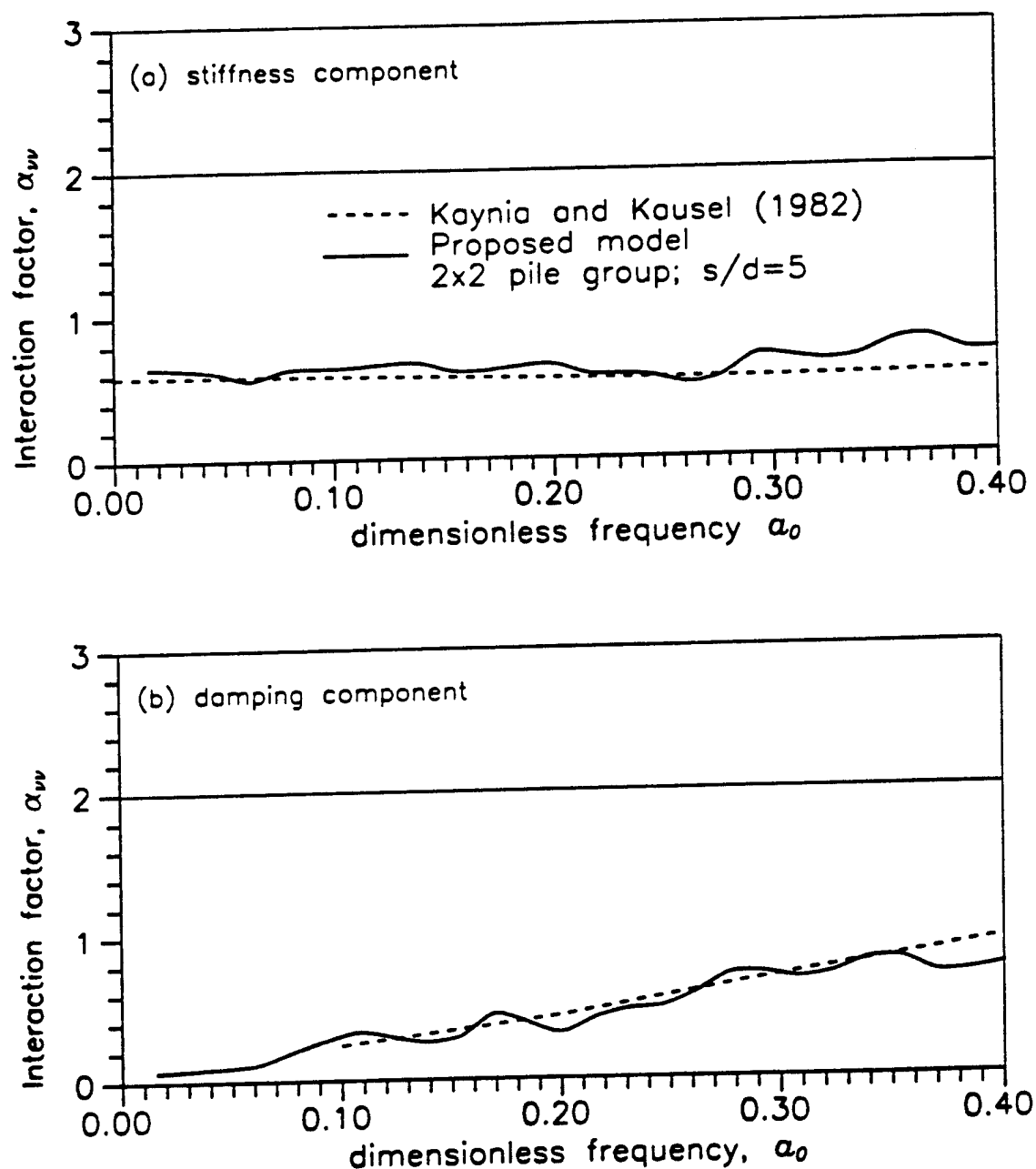


Fig. 5.2: Comparison of dynamic interaction factors, α_w , for stiffness and damping by PILE-3D analysis with factors by Kaynia and Kausel (1982) for 2x2 pile group.

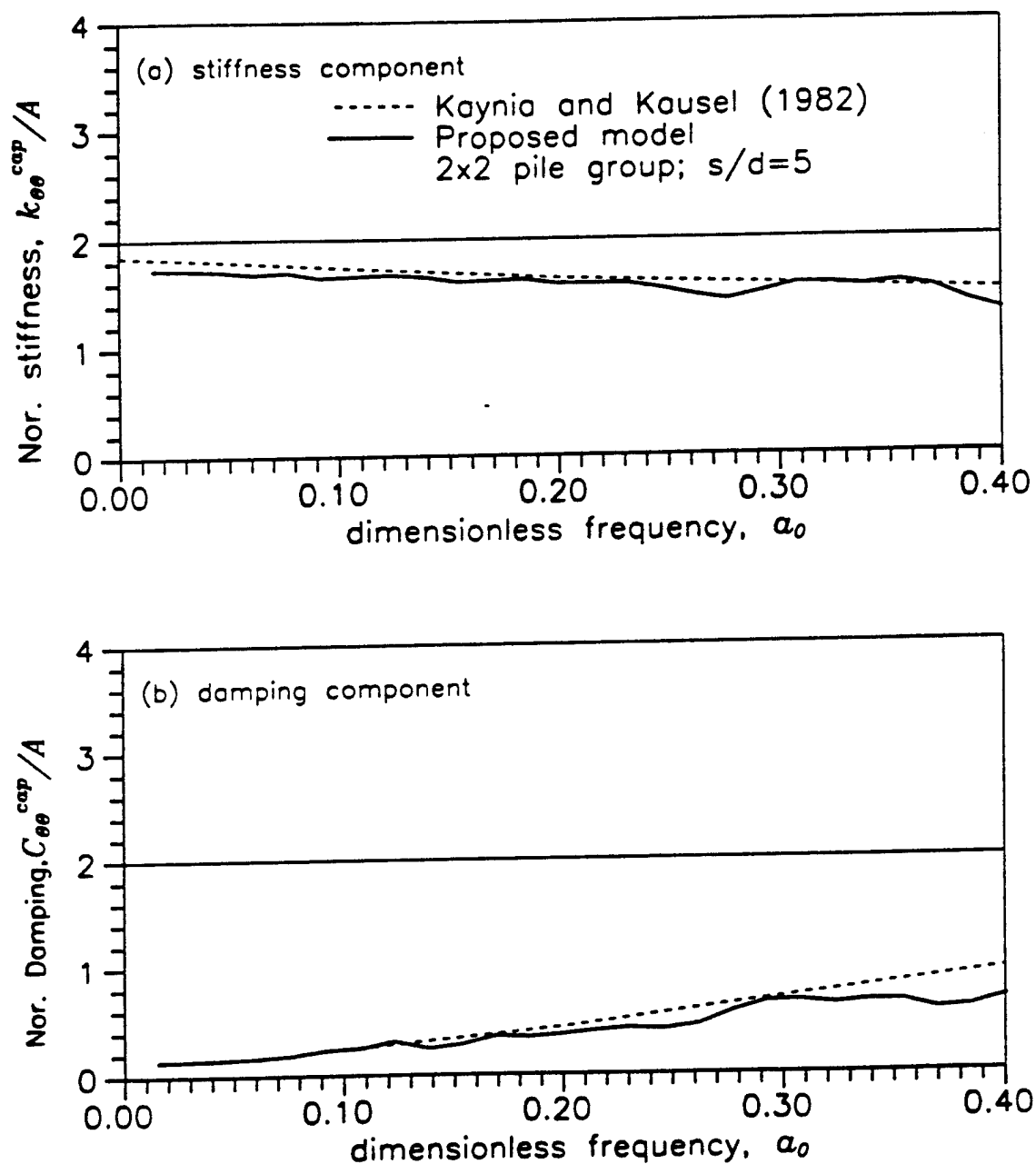


Fig. 5.3: Comparison of dynamic interaction factors, $\alpha_{\theta\theta}$, for rotational stiffness and damping by PILE-3D analysis with factors by Kaynia and Kausel (1982) for 2x2 pile group.

CHAPTER 6

FULL SCALE VIBRATION TEST ON A 6-PILE GROUP

A quick release horizontal vibration test was performed on a full-scale pile group foundation of a large transformer bank (Bank 79) located at the Duwamish Substation, Seattle, Washington (Fig. 6.1). Test data and analytical results were reported by Crouse and Cheang (1987). The foundation of the transformer consists of a pile cap with 6 vertical piles embedded in 40 ft of loose saturated, sandy soils overlying stiff soil.

The test was analyzed using the PILE-3D method of analysis to see how well the computed response could model the field behaviour.

Description of Vibration Test

The transformer and pile foundation (Fig. 6.1) have been described in detail in Crouse and Cheang (1987). The transformer, weighing 326 kips, is anchored to a concrete pedestal which is a continuous part of the pile cap. The pile cap has dimensions of 13.4 ft by 8.00 ft. The pile cap is embedded beneath the ground surface as shown in Fig. 6.1. The pile foundation consists of 6 vertical concrete filled steel pipe piles, each 12 inches O.D. with a wall thickness of 0.172 ins.. These piles are spaced at 4.67 ft and 5.00 ft centre to centre in the X and Y directions, respectively. All the piles are extended into the very dense glacial till layer at the 40 ft depth. The composite axial rigidity (EA) and flexural rigidity (EI) of each concrete filled pipe pile are 5.1×10^8 lb and 4.24×10^7 lb.ft², respectively, where E = Young's modulus, A = cross-sectional area, and I = moment of inertia.

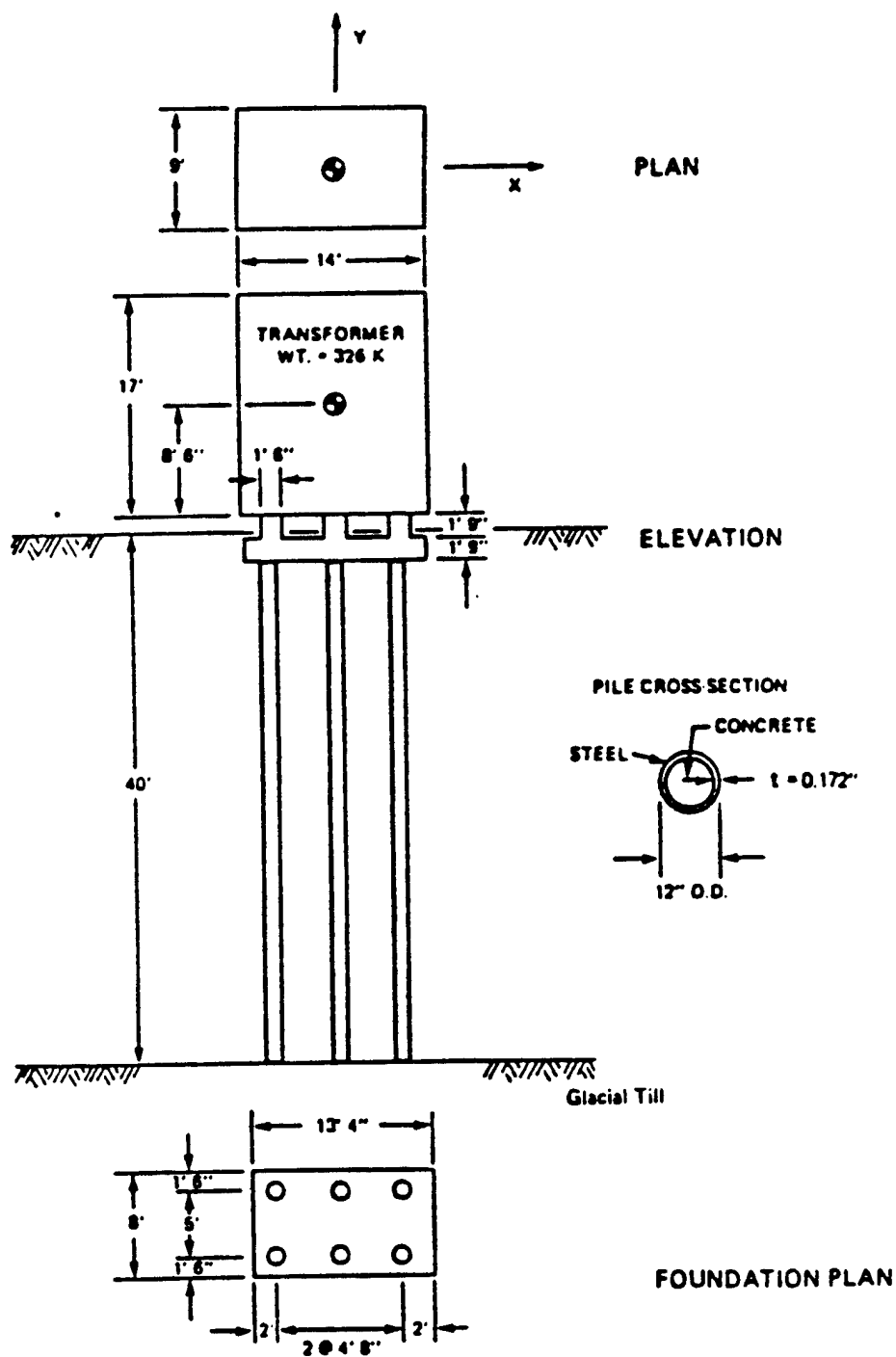


Fig. 6.1. Transformer mounted on pile foundation.

Figure 6.2 shows the idealized soil profile at Duwamish Station according to Crouse and Cheang (1987). The soil profile consists of mostly loose to medium-dense sand to silty sand, with some dense sand or gravelly sand layers overlying very dense gravelly sand glacial till at a depth of 12.2 m. The groundwater table is at a depth of 3.7 m. The in-situ shear wave velocities (V_s), measured by a downhole seismic survey, are 125 m/sec in the upper 3.7 m and 165 m/sec below 3.7 m depth.

The quick-release free vibration test was conducted by Crouse and Cheang (1987). A sling, attached to the transformer, was pulled and quickly released to let the structure vibrate freely. The motions were recorded at various locations on the foundation. Tests were performed in the direction of both principal horizontal axes of the transformer foundation. The Y-axis is in the NS direction; the X-axis is in the EW direction. The resonant frequencies and damping ratios of the transformer foundation system were determined from the recorded time histories of transient vibrations by Crouse and Cheang (1987). The measured fundamental frequencies in NS and EW directions are 3.8 Hz and 4.6 Hz, respectively. The corresponding damping ratios are 6% and 5%.

Computed Results using PILE-3D

The soil profile shown in Fig. 6.2 was used except that the shear modulus distribution proposed by Sy (1992) was adopted. Sy (1992) made a correction to measured shear wave velocity to account for the soil densification due to pile installation. An increase of 4% in low strain shear modulus G_{\max} values was applied to the measured free-field values for this correction. Poisson's ratio $\nu = 0.3$ and material damping ratio $\lambda = 5\%$ are used for all soil layers in the present analysis. This level of material damping is assumed to be reasonable for the low level of

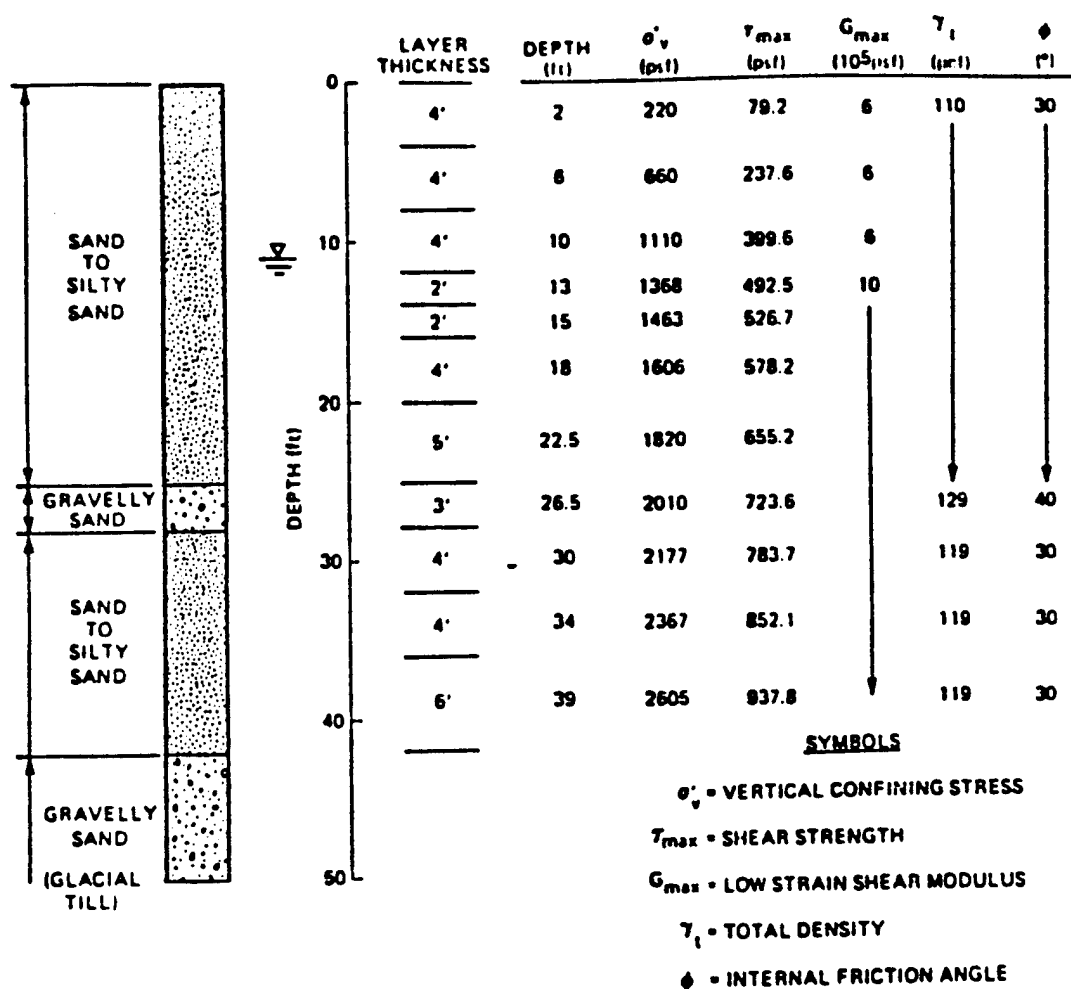


Fig. 6.2: Idealized soil profile at Duwamish Substation (after Crouse and Cheang, 1987).

excitation. If a nonlinear analysis were performed as described in the next chapter, the variable damping level would be calculated by the program from the inputted information on the strain-dependency of the damping. Figures 6.3(a) and (b) show the finite element models used in the analysis.

The resonant frequencies of the transformer-pile cap system are determined from the computed dynamic response of the system to horizontal harmonic forced excitation at different frequencies. The computed and measured resonant frequencies and damping ratios, are given in

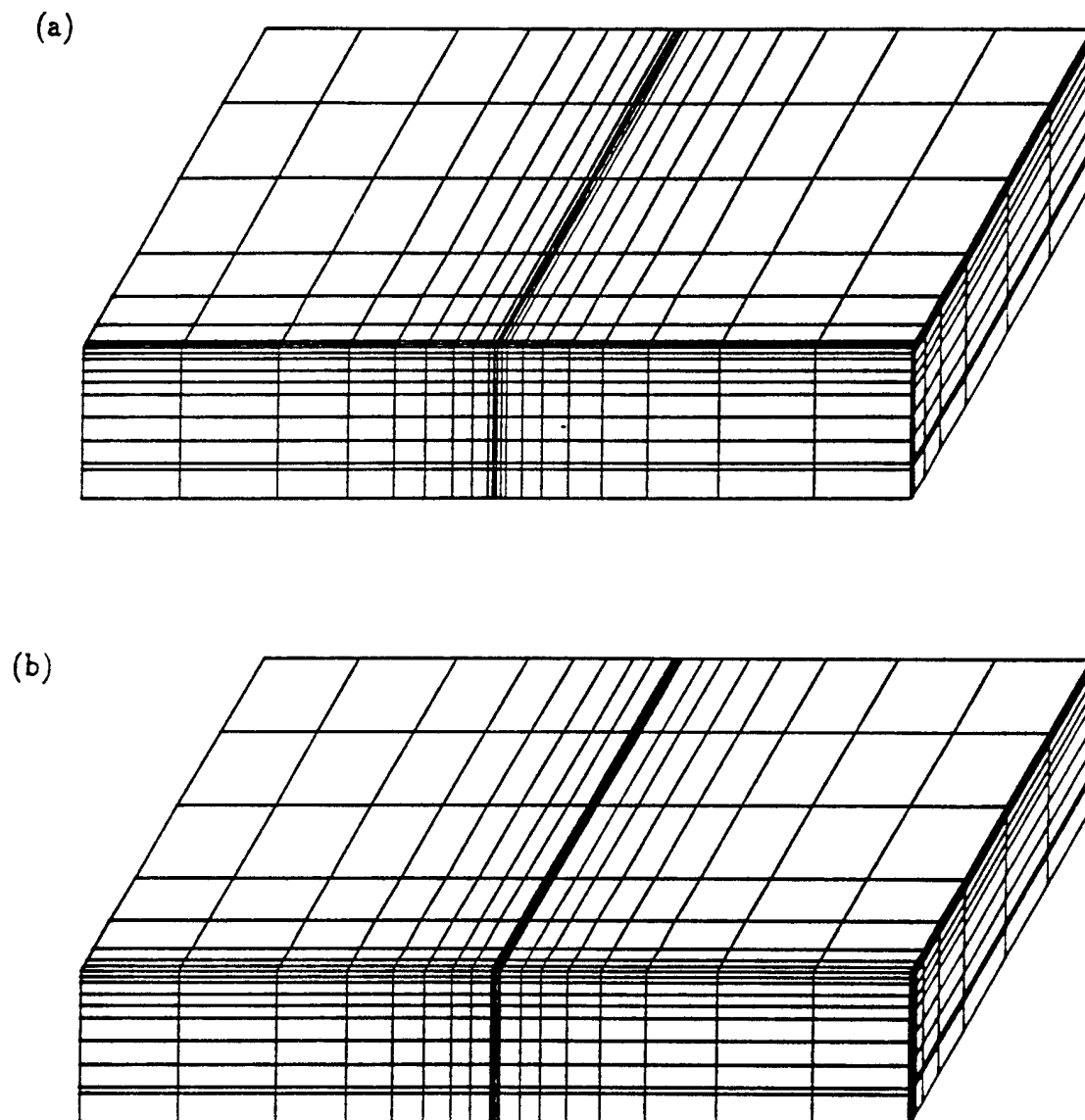


Fig. 6.3: 3-D finite element models of the 6-pile foundation (a) NS direction, (b) EW direction.

Table 6.1. The computed values were determined without taking into account the effect of pile cap embedment.

Table 6.1: Computed Resonant Frequencies and Damping Ratios Without the Effect of Pile Cap Embedment.

Resonant Frequencies (Hz)				Damping Ratios			
Computed		Measured		Computed		Measured	
NS	EW	NS	EW	NS	EW	NS	EW
3.50	4.37	3.8	4.60	0.08	0.06	0.06	0.05

Effect of Pile Cap Embedment

According to Crouse and Cheang (1987), gaps may exist between the pile cap and the soil underneath due to settlement of soil. Conventionally the effect of pile cap-soil interaction has been included by considering the soil reaction acting on the vertical sides of the pile cap (Prakash and Sharma, 1990; Novak et al., 1990). Therefore, in this analysis, only the soil reactions acting on the vertical sides of the pile cap are included. The side reactions due to pile cap embedment usually result in increased foundation stiffness and damping. According to Beredugo and Novak (1972), the foundation stiffness and damping due to pile cap embedment can be determine using a plain strain soil model.

The rectangular pile cap had an area of 106.67 ft^2 and an equivalent radius of 5.83 ft. The embedment depth of the pile cap was 1.75 ft, and the average shear modulus of soil over that depth was $6.0 \times 10^5 \text{ psf}$. Based on these data, using Beredugo and Novak's (1972) solution, the stiffness and damping due to pile cap embedment are determined at the bottom of the pile cap to be:

Translation:

$$k^*_{ww} = 4.20 \times 10^6 \text{ lb/ft}$$

$$C^*_{ww} = 1.33 \times 10^3 \times \omega \text{ lb/ft}$$

Cross-Coupling:

$$k^*_{v\theta} = 3.68 \times 10^6 \text{ lb/rad}$$

$$C^*_{v\theta} = 1.16 \times 10^5 \times \omega \text{ lb/rad}$$

Rotation:

$$k^*_{\theta\theta} = 9.34 \times 10^7 \text{ lb.ft/rad}$$

$$C^*_{\theta\theta} = 1.03 \times 10^6 \times \omega \text{ lb.ft/rad}$$

The total stiffness and damping factors for the transformer foundation are obtained by adding the stiffness and damping factors due to pile cap embedment to those of the pile group. The total factors and the factors without embedment are shown in Table 6.2 at the resonant frequencies of the system. The pile cap embedment results in changes in stiffness less than 25%. Changes in the damping are very significant as would be expected.

Table 6.2: Computed Stiffness and Damping of the Transformer Pile Foundation.

	N-S (f = 3.74 Hz)		E-W (f = 4.63 Hz)	
	With embed. effect	Without embed. effect	With embed. effect	Without embed. effect
k_{ww} (lb/ft)	2.46 E+7	2.04 E+7	2.55 E+7	2.13 E+7
$k_{v\theta}$ (lb/rad)	-2.21 E+7	-2.57 E+7	-2.43 E+7	-2.79 E+7
$k^{\text{cap}}_{\theta\theta}$ (lb.ft/rad)	1.34 E+9	1.25 E+9	2.59 E+9	2.50 E+9
C_{ww} (lb/ft)	10.0 E+6	7.05 E+6	8.81 E+6	5.05 E+6
$C_{v\theta}$ (lb/rad)	-5.10 E+6	-7.62 E+6	-1.97 E+6	-5.25 E+6
$C^{\text{cap}}_{\theta\theta}$ (lb.ft/rad)	9.20 E+7	6.91 E+7	1.74 E+8	1.44 E+8

The dynamic response curves of the transformer-pile cap system were computed for the two cases; including and excluding the effect of pile cap embedment. Figure 6.4 shows the computed dynamic response curves of the transformer-pile cap system for both cases. The measured fundamental frequencies are shown by the vertical lines.

The computed and measured resonant frequencies and damping ratios of the transformer-pile cap system including the effects of pile cap embedment are given in Table 6.3. The computed resonant frequencies are 3.74 Hz and 4.63 Hz in the NS direction and in the EW directions, respectively. The corresponding measured resonant frequencies are 3.8 Hz and 4.6 Hz. The computed resonant frequencies match very well with the measured frequencies in both principal directions.

Table 6.3: Measured and Computed Resonant Frequencies and Damping Ratios Including the Effect of Pile Cap Embedment.

Natural Frequencies (Hz)				Damping Ratios			
Computed		Measured		Computed		Measured	
NS	EW	NS	EW	NS	EW	NS	EW
3.74	4.63	3.8	4.60	0.09	0.09	0.06	0.05

The damping, however, is now overestimated. The computed damping in this case is uncertain because the system was analyzed as an elastic solid with radiation and material damping, and a somewhat arbitrary damping ratio of 5% was included to model the hysteretic material damping of the soil. Using nonlinear techniques to be described later, the correct material damping will be computed directly by the program.

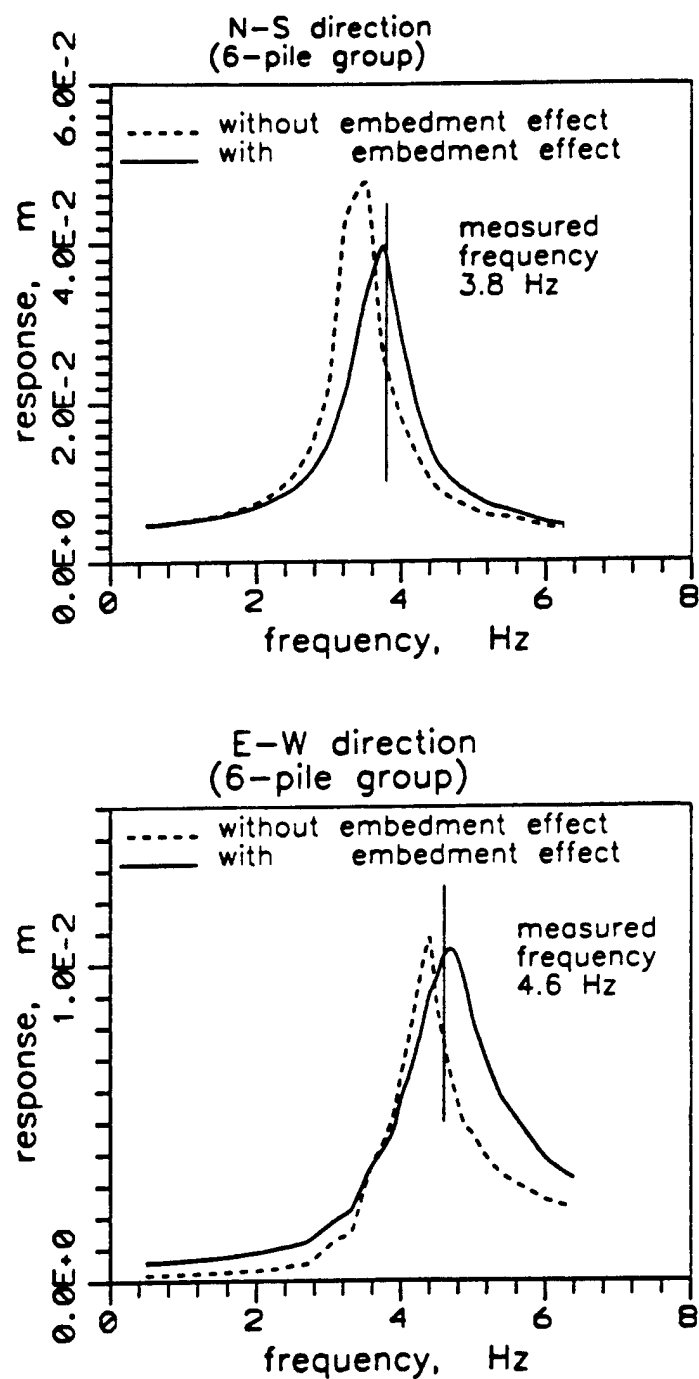


Fig. 6.4: Response curves of the transformer-pile cap system (a) NS direction, (b) EW direction.

CHAPTER 7

NONLINEAR DYNAMIC RESPONSE ANALYSIS OF PILES

The equations of motion are given by the incremental form by

$$[M]\{\Delta\ddot{v}\} + [C]\{\Delta\dot{v}\} + [K]\{v\} = \{P(t)\} = -[M][I] \Delta\ddot{v}_b(t) \quad (7.1)$$

Analysis of nonlinear response must be conducted in the time domain. The direct step by step integration procedure developed by Wilson et al. (1973) is used to integrate the equations of motion.

Rayleigh damping is used to model the hysteretic damping of the soil for nonlinear analysis. The damping element matrix is given by

$$[C]_{\text{elem}} = \alpha[M]_{\text{elem}} + \beta[K]_{\text{elem}} \quad (7.2)$$

in which α and β are constants related to the viscous damping ratio for the element. Let

$$\alpha = \lambda_{\text{elem}} / \omega_1 \quad \text{and} \quad \beta = \lambda_{\text{elem}} / \omega_1 \quad (7.3)$$

where λ_{elem} is the damping ratio corresponding to element shear strain and ω_1 is the fundamental frequency of the system (Idriss et al., 1974).

The global damping matrix $[C]$ is the aggregate of all the element damping ratios and the radiation damping elements along the pile.

For nonlinear analysis because of integration in the time domain, it is more efficient to use a diagonal mass matrix rather than the consistent mass matrix used earlier. Therefore, the mass matrices for soil and beam elements, $[M]_{\text{soil}}$ and $[M]_{\text{beam}}$, respectively, are now given by

$$[M]_{\text{soil}} = \frac{\rho_s \cdot \text{vol}}{8} \{1.0, 1.0, 1.0, 1.0, 1.0, 1.0, 1.0, 1.0\} \quad (7.4)$$

and

$$[M]_{\text{beam}} = \rho_p A \ell \{1/2, 1/78, 1/2, 1/78\} \quad (7.5)$$

Soil modulus and damping in soils are shear strain dependent (Seed and Idriss, 1970). For nonlinear analysis using PILE-3D, the strain-dependence of effective shear modulus and damping must be specified for the different materials in the foundation soils. During analysis, compatibility is maintained between the instantaneous computed shear strains and the effective modulus and damping in each finite element. The compatibility can be restored for each time increment during integration of the equations of motion or at specified times which are multiples of the time increment for integration. This procedure differs from the equivalent linear method used in programs such as SHAKE (Schnabel et al., 1972) in which compatibility is enforced only after the complete response analysis has been carried out. Ensuring final compatibility in that case requires iterative analysis using the entire duration of the earthquake in each analysis. No iterative analyses are required when compatibility is enforced during the analysis as in PILE-3D.

Two other features distinguish the nonlinear model proposed here from the Schnabel et al. (1972) model. Shear yielding is incorporated by introducing a very low modulus when the

strength of the soil is reached. No tensile stresses are allowed. This is accomplished by introducing a very low modulus when the normal stress in any direction tends to become greater than the tensile strength of the soil if any. The details of this kind of analysis will be illustrated by the analysis of a pile group in sand under strong shaking in a centrifuge test.

CHAPTER 8

DYNAMIC ANALYSIS OF CENTRIFUGE TEST OF A PILE GROUP

Description of Centrifuge Test on a Four-Pile Group (2×2)

A centrifuge test on a four-pile (2×2) group was conducted by Gohl and reported by Finn and Gohl (1987) and Gohl (1991). The test set-up is shown in Fig. 8.1. The piles were set in a 2×2 arrangement at a centre-to-centre spacing of 2 pile diameters or 1.14 m. Two of the four piles were instrumented. The piles were rigidly clamped to a stiff pile cap, and four cylindrical masses were bolted to the cap to provide additional inertia. A pile cap accelerometer and a displacement L.E.D. were placed at locations shown in the figure. The displacement L.E.D. was located 46 mm (2.76 m in prototype scale) above the four pile heads.

At prototype scale, the pile cap has a mass of 220.64 kN.sec²/m and a mass moment of inertia about centre of gravity $I_{cv} = 715.39$ kN.sec²/m. The centre of gravity was 0.96 m above the pile-head. The piles had a free standing length of 1.21 m above the soil surface.

The sand used for the pile group test was a dry dense sand with a void ratio $e_0 = 0.57$ and a mass density $\rho = 1.70$ Mg/m³. The friction angle of the dense sand was 45°. Gohl (1991) showed that the small strain shear modulus G_{max} can be evaluated using the Hardin and Black (1968) equation with a lateral stress coefficient $K_0 = 0.6$.

The four pile group was shaken by a simulated earthquake acceleration motion. Peak accelerations of up to 0.14 g were applied to the base of the foundation and were dominated by frequencies in the range of 0 to 5 Hz. The free-field accelerations were strongly amplified through the sand deposit to values of up to 0.26 g at the surface. Pile cap accelerations of up to

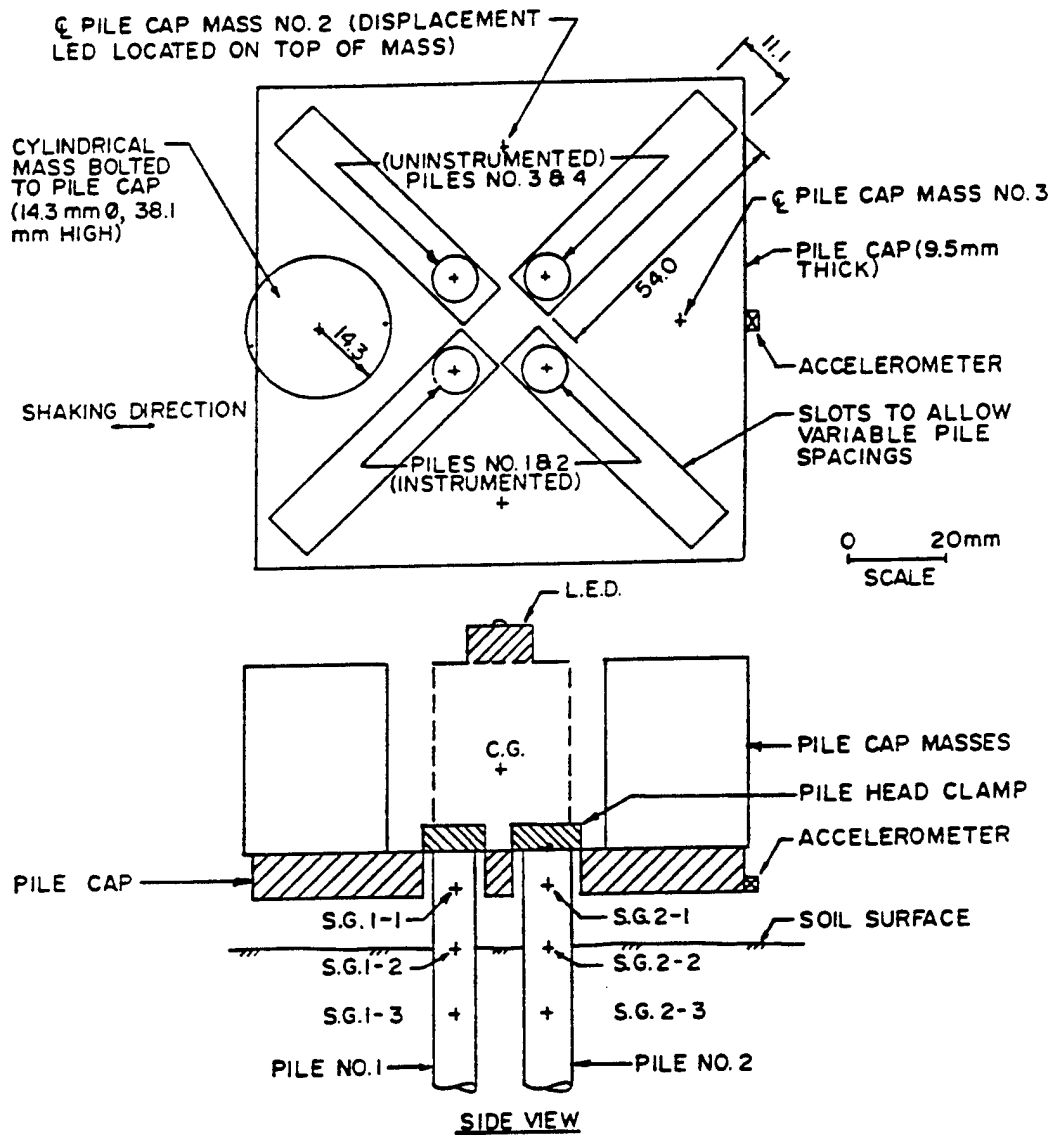


Fig. 8.1: The layout of centrifuge test for four-pile group (after Gohl, 1991).

0.24 g and displacements up to 60 mm were recorded during the test. Residual displacements of up to 10 mm remained at the end of earthquake motion.

Dynamic Analysis of the Pile Group

In the analysis, the pile cap was treated as a rigid body. Hence all pile heads, which were rigidly connected to the bottom of the pile cap, had had the same translational and rotational displacements as the pile cap.

In PILE-3D, the horizontal motions are uncoupled from the vertical motions. Therefore, the rocking stiffness induced by the vertical resistance of piles cannot be included directly in the analysis of horizontal motions. However, the rocking impedances (resistance) may significantly restrain the rotational motions of the pile caps and, therefore, the effect of rocking impedances on the horizontal motions must be taken into account.

The rocking impedances are computed by performing a series of separate quasi-3D analysis in the vertical mode during the analysis in the horizontal mode. These impedance calculations are made using the current values of strain dependent shear moduli and damping ratios of soil. After the rocking impedances were computed for each time period, they are transferred to the pile cap as rotational stiffness and damping.

The finite element mesh used for analysis with 947 nodes and 691 elements, is shown in Fig. 8.2. The sand foundation was modelled by 11 horizontal layers. Thinner layers were used near the sand surface where pile-soil interaction is strongest. Each pile was modelled using 15 beam elements including 5 elements for the part extending above the soil surface. A very stiff massless beam element was used to connect the structural mass to the pile heads.

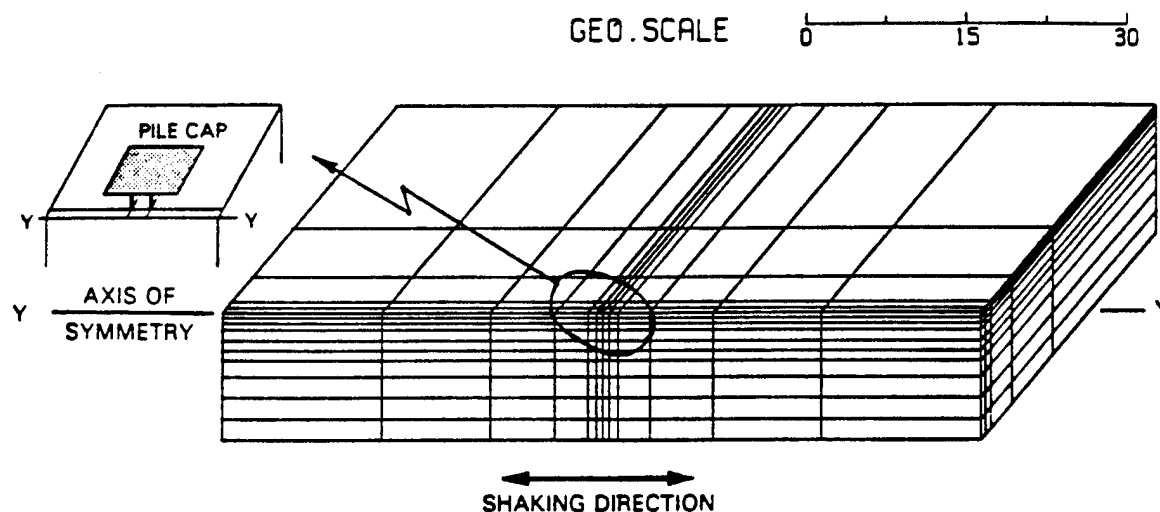


Fig. 8.2: Finite element modelling of the 2x2 pile group.

The analysis was carried out using the nonlinear option in PILE-3D to simulate the changes of shear moduli and damping of soil with the shear strain. The shear-strain dependencies of shear modulus G and damping ratio D for the dense sand are shown in Fig. 8.3 (Gohl, 1991). The small strain shear moduli, G_{\max} , were estimated from shear wave velocities measured in flight using bender elements. The maximum hysteretic damping ratio, D_{\max} , of the sand foundation were taken as 25% following Gohl (1991).

Results of Analysis

Figure 8.4 shows the computed acceleration response at the pile cap versus the measured acceleration response. There is fairly good agreement between the measured and computed accelerations. The computed peak acceleration at the pile cap is 0.23 g which agrees very well with the measured peak acceleration of 0.24 g.

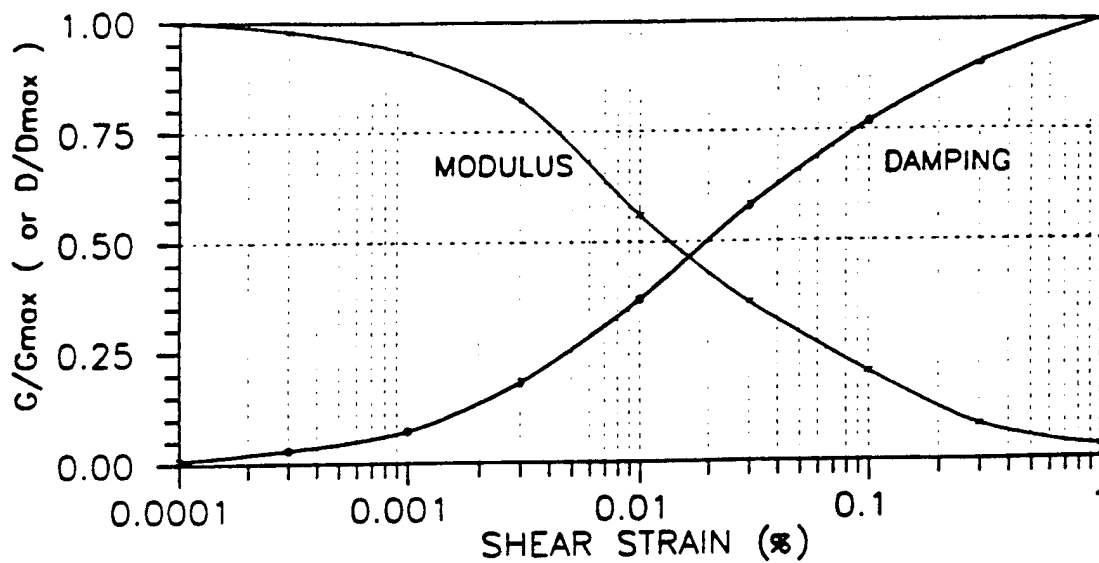


Fig. 8.3: The relationships between shear modulus, damping and the shear strain for the dense sand.

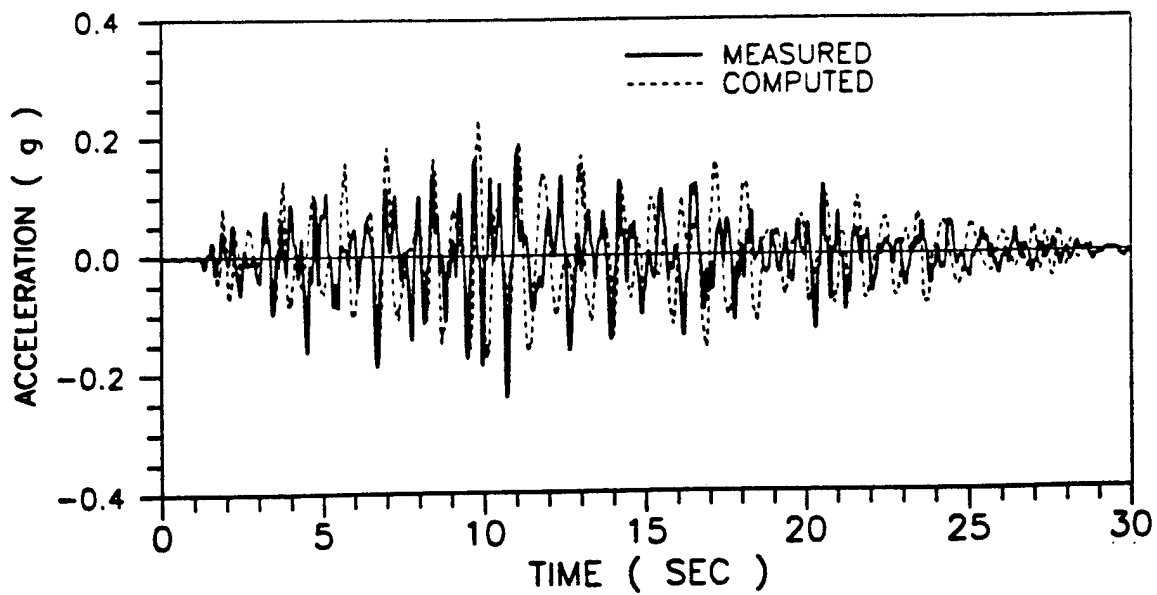


Fig. 8.4: The computed versus measured acceleration responses at pile cap.

The computed displacement at the top of the structural mass matches fairly well with the measured displacement in the first 11 seconds of motion (Fig. 8.5). The computed displacement response did not show any residual displacement, whereas the measured displacement response showed a permanent residual displacement of about 10 mm at the end of the earthquake motion. This is because the analysis is carried out using the equivalent linear elastic approach.

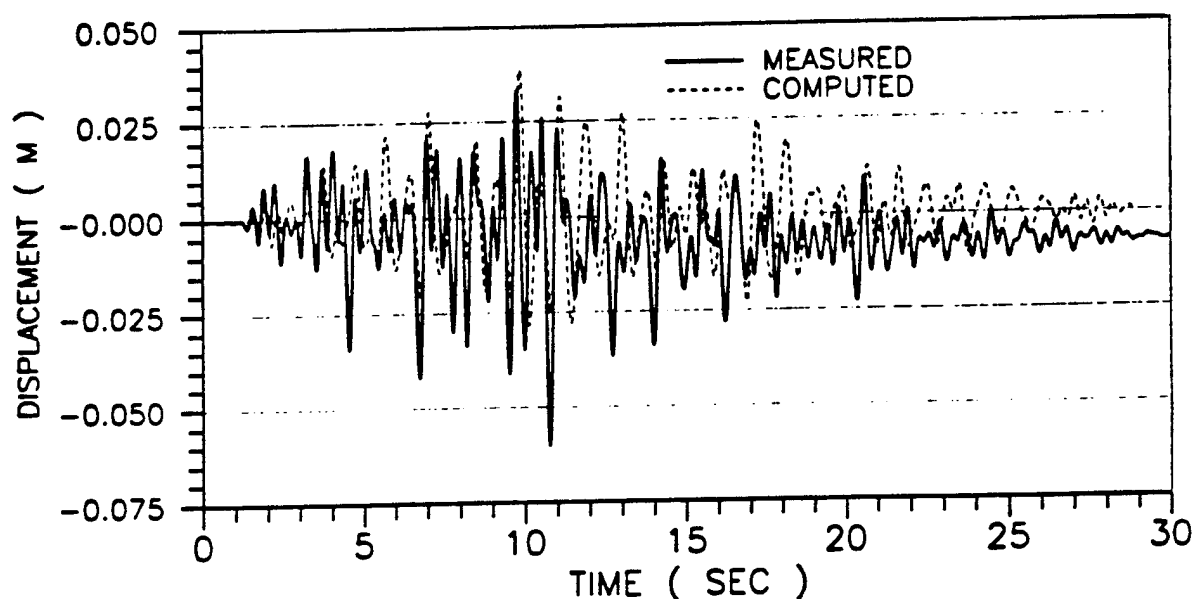


Fig. 8.5: The computed versus measured displacement at the top of the structural mass.

The computed moment time history in the instrumented pile at a depth of 2.63 m (the approximate depth of maximum moment) is plotted against the measured moment time history in Fig. 8.6. There is good agreement between the measured and computed moments. The distribution of computed and measured bending moments along the pile at the instant of peak pile cap displacement are shown in Fig. 8.7. The computed moments agree reasonably well with the measured moments, especially in the region of maximum moments. The computed peak moment is 203 kN/m compared to a measured peak moment of 220 kN/m.

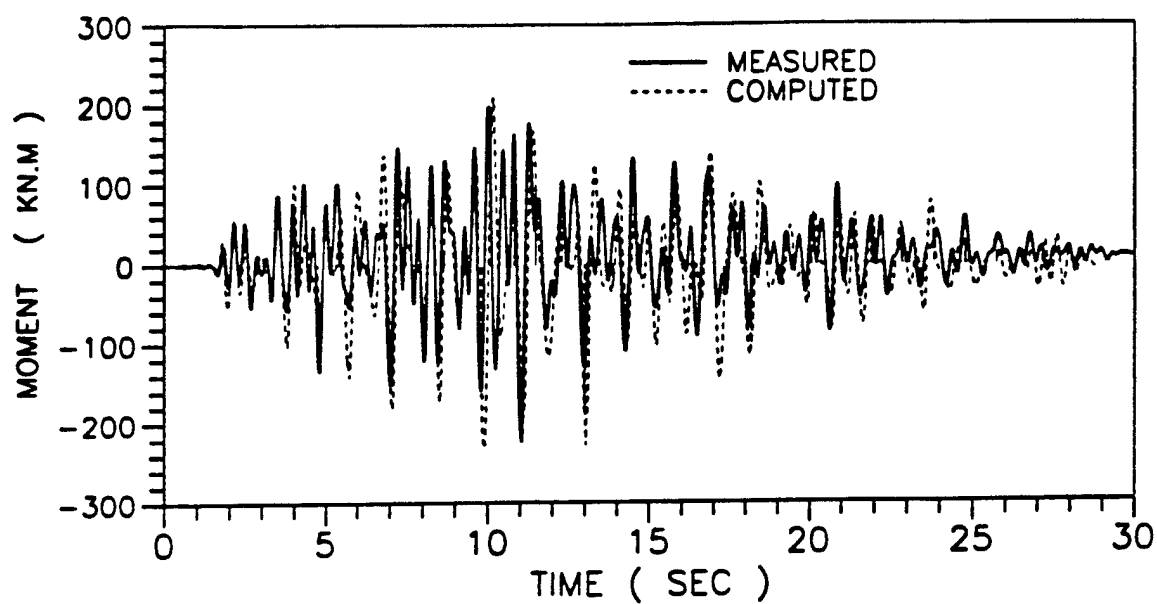


Fig. 8.6: The computed versus measured moment at depth $D = 2.63$ m.

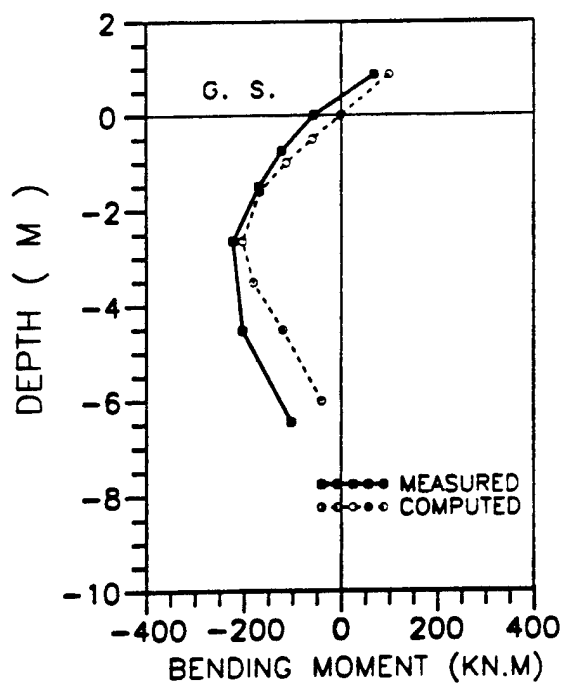


Fig. 8.7: Distribution of moments at peak pile cap displacement.

Nonlinear Impedances of the Four-Pile Group

The variations of stiffnesses K_w and $K_{v\theta}$ of the four-pile group with time are shown in Fig. 8.8 at an excitation frequency $f = 1.91$ Hz. These stiffnesses were calculated at each time instant by the program PILIMP (Wu and Finn, 1994) using the moduli and damping of the soils computed by PILE-3D for that instant of time. This is the first time that it has been possible to calculate the time variation of pile foundation stiffnesses during an earthquake.

It is shown in Fig. 8.8, how dramatically the stiffness changes with the level of excitation. Very large reductions in stiffness occur between 5 and 20 seconds where there is strong shaking. The lateral stiffness K_w decreased to 80,000 kN/m from its initial stiffness of 420,000 kN/rad. The stiffnesses K_w and $K_{v\theta}$ were reduced to about 17% and 38% of their initial stiffnesses. The stiffnesses are larger at the ends of the record where the shaking is at a lower level.

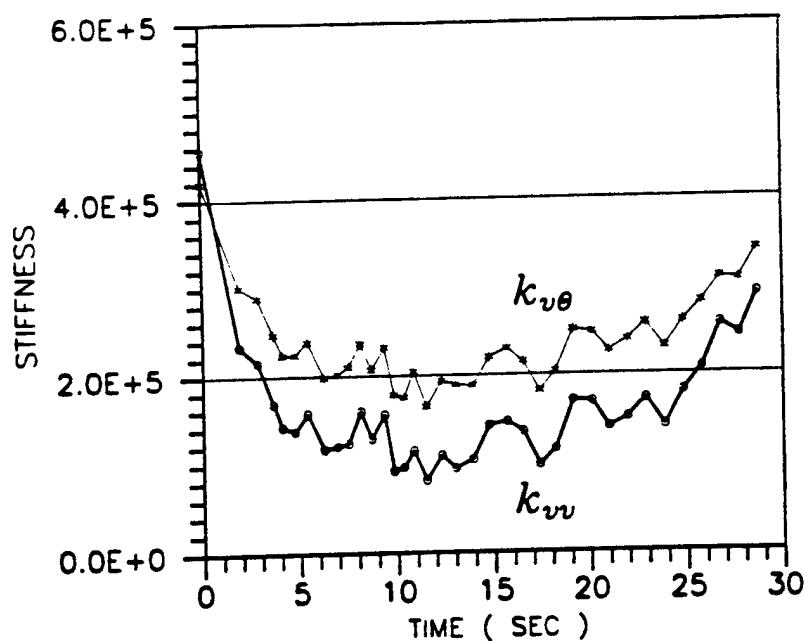


Fig. 8.8: Variation of stiffnesses $k_w, k_{v\theta}$ of the four-pile group at $f = 1.91$ Hz.

CHAPTER 9

CONCLUSIONS AND RECOMMENDATIONS

This study has validated a simplified method for the 3-D analysis of pile foundations (Wu, 1994). The method is of general applicability to the problem of analyzing the effects of inclusions to restrain flow deformations. The validation has been carried out for pile inclusions in the soil because of the wide availability of exact analytical solutions for small pile groups in elastic soil. In addition, field test data on pile foundations and data from simulated earthquake tests on pile foundations in centrifuge tests allow validation of the program for real soils under both low level and strong shaking.

The method of analysis is incorporated in the program PILE-3D (Wu and Finn, 1994). The Phase II report described the validation of the program for the seismic response analysis of single piles. The Phase II report provides more detailed studies and comments on the fundamentals of the analysis. The present Phase III report concentrates on the extension of the method to pile groups. This requires the formulation of the method to include vertical motions of the pile group in order to analyze the rocking motion of a pile group.

The PILE-3D analysis of pile groups was validated in three ways. First, computed dynamic interaction factors for stiffness and damping were compared with factors developed by Kaynia and Kausel (1982) using full 3-D elastic analysis. The comparison was made for a 2×2 pile group. Because of the complexities of the full 3-D analyses, results are available only for small groups. The results from PILE-3D analyses compare very well with the results from the exact analyses. Comparison would be improved by using a finer finite element mesh. However, an important consideration in these analyses is the computational time because it is highly

desirable to conduct parametric studies. Therefore excessive refinements of the analysis is not an effective option for engineering practice.

A field vibration test on a large transformer bank on a pile foundation in Seattle, conducted at low levels of excitation, provided an opportunity to evaluate the program under field conditions. The results were satisfactory. The natural frequencies of the system were very accurately predicted. The analysis was conducted assuming elastic response and so the viscous damping input had to be estimated. Therefore, the damping fit was not good. This problem is removed in nonlinear analysis as the material damping is estimated by the program as a function of shear strain.

The ability of the program to estimate the dynamic response of pile foundations under strong shaking including nonlinear response was validated by simulated earthquake tests on a centrifuged model of a fully instrumented 2×2 pile group. The comparison between computed and measured accelerations, displacements and moments were adequate for engineering purposes. The predicted distribution of peak moments along the piles compared closely with the measured moments.

The extensive validation of the PILE-3D method of analysis suggests that the program is reliable for a wide range in shaking levels and frequency ranges of interest in earthquake engineering. For remediated areas of limited extent using inclusions such as piles or stone columns, the program can estimate response for the 3-D conditions of the problem.

The program has direct application to other problems of interest to the USACE involving pile foundations where it can take into account many of the factors which are currently ignored, such as kinematic and inertial interaction and dynamic interaction between piles and soil during strong shaking.

There is one area that still needs development. To bring the program to its full potential, it is necessary to consider the case where significant porewater pressure or liquefaction can occur during an earthquake. It is recommended that studies for this case be conducted under a final Phase IV research program.

REFERENCES

- Crouse, C.B. and Cheang, L. (1987). "Dynamic Testing and Analysis of Pile-Group Foundations," *Dynamic Response of Pile Foundations - Experiment, Analysis and Observation*, ASCE Geotech. Special Publication No. 11, pp. 79-98.
- Beredugo, Y.O. and Novak, M. (1972). "Coupled Horizontal and Rocking Vibrations of Embedded Footings," *Canadian Geotechnical Journal*, Vol. 9, pp. 477-497.
- Finn, W.D. Liam (1992). "Restraining Post-Liquefaction Flow Deformations," Report to European Research Office of the US Army, London, England.
- Finn, W.D. Liam (1994). "Restraining Post-Liquefaction Flow Deformations - Phase II," Report to European Research Office of the US Army, London, England.
- Finn, W.D. Liam, M. Yogendrakumar, N. Yoshida and H. Yoshida. (1986). "TARA-3: A Program for Nonlinear Static and Dynamic Effective Stress Analysis," Soil Dynamics Group, University of British Columbia, Vancouver, B.C., Canada.
- Finn, W.D. Liam and W.B. Gohl. (1987). "Centrifuge Model Studies of Piles Under Simulated Earthquake Loading," from *Dynamic Response of Pile Foundations - Experiment, Analysis and Observation*, ASE Convention, Atlantic City, New Jersey, Geotechnical Special Publication No. 11, pp. 21-38.
- Finn, W.D. Liam and M. Yogendrakumar. (1989). "TARA-3FL - Program for Analysis of Liquefaction Induced Flow Deformations," Department of Civil Engineering, University of British Columbia, Vancouver, B.C., Canada.
- Finn, W.D. Liam, R.H. Ledbetter, R.L. Fleming Jr., A.E. Templeton, T.W. Forrest and S.T. Stacy. (1991). "Dam on Liquefiable Foundation: Safety Assessment and Remediation," *Proceedings, 17th International Congress on Large Dams*, Vienna, pp. 531-553, June .
- Gohl, W.B. (1991). "Response of Pile Foundations to Simulated Earthquake Loading: Experimental and Analytical Results," Ph.D. Thesis, Dept. of Civil Engineering, University of British Columbia, Vancouver, B.C., Canada.
- Hardin, B.O. and W.L. Black, (1968). "Vibration Modulus of Normally Consolidated Clay," *ASCE, J. Soil Mechanics and Foundations Division*, Vol. 94, pp. 353-369.
- Idriss, I.M., H.B. Seed and N. Serff, (1974). "Seismic Response by Variable Damping Finite Elements," *Journal of Geotechnical Engineering Division, ASCE*, Vol. 100, No. 1, pp. 1-13.
- Kaynia, A.M. and E. Kausel. (1982). "Dynamic Behaviour of Pile Groups," *2nd Int. Conf. on Num. Methods in Offshore Piling*, Austin, TX, pp. 509-532.

Novak, M, Sheta, M., El-Hifnawy, L., El-Marsafawi, H. and Ramadan, O. (1990). "DYNA3, A Computer Program for Calculation of Foundation Response to Dynamic Loads - User's Manual," Geotech. Research Centre, The University of Western Ontario, London, Ontario, Canada.

Novak, M. (1991). "Piles Under Dynamic Loads," State of the Art Paper, 2nd Int. Conf. on Recent Advances in Geotech. Earthq. Eng. and Soil Dyn., University of Missouri-Rolla, Rolla, Missouri, Vol. III, pp. 250-273.

Prakash, S. and Sharma, H.D. (1990). "Pile Foundation in Engineering Practice," John Wiley & Sons, Inc.

Schnabel, P.B., J. Lysmer and H.B. Seed (1972). "SHAKE: A Computer Program for Earthquake Response Analysis of Horizontally Layered Sites," Report EERC 71-12, University of California at Berkeley.

Seed, H.B. and I.M. Idriss, (1970). "Soil Moduli and Damping Factors for Dynamic Response Analyses," Report No. EERC 70-10, Earthquake Engineering Research Center, University of California, Berkeley, California.

Sy, A. (1992). "An Alternative Analysis of Vibration Tests on Two Pile Group Foundations," Piles Under Dynamic Loads, ASCE Geotech. Special Publication No. 34, pp. 136-152.

Sy, A. and D. Siu, (1992). "Forced Vibration Testing of An Expanded Base Concrete Pile," Piles Under Dynamic Loads, ASCE Geotech. Special Publication No. 34, 170-186.

Wood, J.H. (1973). Earthquake-Induced Soil Pressures on Structures. Ph.D. Thesis, submitted to the California Institute of Technology, Pasadena, California.

Wilson, E.L., L. Farhoomand and J.K. Bathe (1973). Nonlinear Dynamic Analysis of Complex Structures. International Journal of Earthquake Engineering and Structural Dynamics, Vol. 1, No. 3, Jan-March.

Wu, Guoxi (1994). "Dynamic Soil-Structure Interaction: Pile Foundations and Retaining Structures," Ph.D. Thesis, Department of Civil Engineering, University of British Columbia, Vancouver, B.C., October, 198 pages.

Wu, G. and W.D. Liam Finn (1994). PILE-3D - Prototype Program for Nonlinear Dynamic Analysis of Pile Groups, (still under development), Department of Civil Engineering, University of British Columbia, Vancouver, B.C.

Wu, G. and W.D. Liam Finn (1994). PILIMP - Prototype Program for Determining the Impedances of Piles and Pile Groups for a Specified Distribution of Soil Properties, Department of Civil Engineering, University of British Columbia, Vancouver, B.C.